

Detection of transient signals based on the tricepstrum

Christos K. Papadopoulos ^{*}, George Ch. Ioannidis, Constantinos S. Psomopoulos

Piraeus University of Applied Sciences, Dept. of Electrical Engineering, GR-122 44, Egaleo, Greece



ARTICLE INFO

Article history:

Available online 7 March 2018

Keywords:

Detection
Transient signals
Tricepstrum
Energy detector
Adaptive

ABSTRACT

In this paper, the problem of detecting transient signals of unknown waveforms and arrival times embedded in white Gaussian noise is addressed. The use of the cepstrum coefficients of the fourth order correlations of the transient signal for forming a detection statistic is demonstrated. It is considered both a batch and adaptive approach for the detection of the signal which is assumed to satisfy a linear constant coefficient difference equation. The adaptive approach is a least squares realization based on Q-R decomposition of the fourth order statistics matrix involved in the computation of the cepstrum coefficients. Their performance is compared in terms of probability of detection and probability of false alarm with the conventional energy detector by means of Monte-Carlo simulations and improved performance is demonstrated. It is shown that the adaptive approach allows for detection of short length transients which are of unknown arrival times using a single data record even before the whole amount of data becomes available. The Q-R decomposition offers good numerical properties when fourth order statistics are involved and in contrast to the energy detector the proposed receiver has false alarm rate independent of the noise if it is of zero mean and independent, identically, distributed (i.i.d.).

© 2018 Elsevier Inc. All rights reserved.

1. Introduction

Detection of transient signals of unknown waveforms and unknown arrival times is a common problem in several signal processing areas. It finds applications in the detection of seismic signals where the array consists of geophone sensors, the detection of acoustic signals in the ocean using hydrophone arrays and also in radar. Transients can be either deterministic or stochastic signals, are short in duration, embedded in long periods of background noise. In both cases we have a highly non-stationary problem. Classical signal detection theory has been applied to this problem mainly using the autocorrelation or data domain [1,2]. The main assumption is that the signal and noise statistics are accurately known either in terms of the probability density functions involved or in terms of the spectra of the signals and noise.

For the case when the signal is stochastic a lot of work has been done for the parametrization of the spectrum using autoregressive (AR) or autoregressive-moving average (ARMA) models, however, the use of these techniques in the detection problems has been limited. Most of the work available involves algorithms for detecting narrow-band signals (sinusoids) embedded in complex white Gaussian noise [3–6].

Higher order statistics have been used for spectrum estimation of stochastic signals [7–19]. For detection problems their use has not been very extensive. In [20] the complex version of the multivariate T-test is used to detect non-Gaussian signals in Gaussian noise. The detector is suboptimum, motivated by the fact that the estimated bifrequency pairs are asymptotically normal and statistically independent random variables. However, it performs a maximum likelihood ratio (LRT) in the bispectrum domain. In [21] the bispectrum is also used to detect the presence of nonlinear and non-Gaussian time series in the presence of Gaussian noise. The detector here also uses the bifrequency pairs by taking the sum of the squares normalized by the variance expressed as the skewness of the bispectrum. The main motivation for using higher order statistics for detection purposes lies in their ability to suppress noise under certain conditions. For example, for the case of zero mean Gaussian noise all cumulants of order three and above are zero, i.e., cumulant domains or cumulant spectra may become high Signal to Noise Ratio (SNR) domains, in the cases where the higher-order spectrum of the signal is non-zero.

Here the interest lies in using transient signals whose waveforms and arrival times are unknown. If the deterministic signal waveform is unknown but the arrival time is known and the signal is embedded in additive white Gaussian noise, a generalized likelihood ratio test is discussed in [1] where the signal is the impulse response of a proper rational transfer function. However, the implementation of the test is obtained at the expense of solving a

^{*} Corresponding author.

E-mail address: cp26041960@gmail.com (C.K. Papadopoulos).

set of non-linear equations even for the simple case of a second-order transfer function, which means that some a-priori knowledge for the signal is required. Furthermore, the detector is not of constant false alarm rate (CFAR) and for the case of unknown noise variance it is difficult to predict the detection performance because the probability density functions under H_0 and H_1 hypothesis turn out to be ratio of quadratic forms. A similar approach is presented in [22] where the noise is colored Gaussian AR(M) process. After estimating the order of the signal model and the AR parameters of the noise process the same test statistic as in [1] is used. For the same transient problem but for unknown arrival times the Gabor representation of the signals is used in [2]. The Gabor coefficients are grouped into a single vector and the multivariate T-test is used. All the above approaches to the problem assume that the deterministic transient signal can be represented as a superposition of damped exponential sinusoids. A different approach is taken in [23] where the assumption for the transient is that it is bandlimited. The test is based on the property of the discrete time bispectrum [24], that for every bandlimited stationary signal there is a region of its principal domain where the bispectrum must be zero. Detection of the signal is accomplished whenever the bispectrum in this region is not zero. No further assumptions are made for the signal and for the noise, the stationarity requirement is enough.

In radar and sonar, transient signal detection plays an important role in detecting targets. Active and passive systems receive a transient signal from which we estimate parameters such as direction of arrival and target distance in cases where the signal's wave shape is known or not. In underwater passive surveillance systems transient sounds are harder to disguise and are becoming more useful for detecting targets. In the naval scenario, quick and accurate detection of transient signals offers an advantage of longer response time to thwart an enemy attack. Also in those applications, ideal signals are usually contaminated with non-Gaussian noise. The radar performance can be degraded by impulsive noise interference such as environmental effects of atmospherics (lightning) and meteor train echoes.

In hydraulic and power systems transient signals monitoring protects the system. The major issue is that these signals reflect a sudden change of the dynamical system which can cause, in an unpredictable lap of time, a breakdown of the system. For example, the electrical partial discharge (PD) detection and characterization. The PDs indicate that some changes have occurred in the insulation due to chemical and/or mechanical transformations, which, in time, can lead to the failure of the equipment. Hereby, the PD measurement is a routine procedure for testing important components from the power system (high-voltage cables, transformers, etc.). Another application concerns the detection, localization and characterization of electrical arcs generated in photovoltaic panels. The need of detection, localization and characterization of the electrical arcs is a growing demand as these systems continue to develop and the environmental conditions still unexpectedly change.

In hydraulic systems, transient signal detection finds application to the water hammer effect which appears in pipelines when a valve is suddenly closed, so it forces the fluid to change its direction or to stop its flow. This translates to a pipe pressure sudden increase/decrease which causes from vibrations of the pipe to system collapse. Thus, this phenomenon must be supervised and characterized in order to control its damaging effects to the hydraulic system.

In the detection of seismic waves, and in biomedicine where the signal carries important information of the disease and an early detection is essential for the treatment.

Here it is proposed a new detection scheme for the detection of transient signals based on the computed cepstrum coefficients of the fourth-order statistics of the signal [15]. Cepstrum coefficients

are appropriate for representation of transient signals because they contain all the information of the signal. Since they also peak around the origin they are suitable for signal detection. The proposed method is capable of detecting transient signals of unknown arrival times. Furthermore, it does not require knowledge of the noise variance or skewness and it is also able to detect the signal in the presence of non-Gaussian white noise. The paper is organized as follows. In section 2, a batch and a recursive approach is presented for the proposed detector. In section 3, its performance is demonstrated by means of simulation examples. Finally conclusions are drawn in section 4.

2. The use of cepstrum coefficients for the detection of transient signals

2.1. The higher order cepstrum based detector

The following detection problem is considered

$$\begin{aligned} H_0: \quad & x(n) = w(n) \\ H_1: \quad & x(n) = m(n) + w(n), \quad n = 0, \dots, N-1 \end{aligned} \quad (1)$$

where $w(n)$ is a stationary, zero mean, white, Gaussian noise of unknown variance σ_w^2 and $m(n)$ is a deterministic transient signal of unknown waveform. The complex cepstrum of the fourth order statistics of a random process $\{x(n)\}$ is known to satisfy the following identity [15],

$$\begin{aligned} & \sum_{k=1}^p A(k) [f_x(-(m+k), -m, -m) \\ & \quad - f_x(-(m-k), -(m-k), -(m-k))] \\ & + \sum_{k=1}^q B(k) [f_x(-(m+k), -(m+k), -(m+k)) \\ & \quad - f_x(-(m-k), -m, -m)] \\ & = m \cdot f_x(-m, -m, -m) = c_x(-m, -m, -m) \\ & \times p, q \rightarrow \infty \end{aligned} \quad (2)$$

where the minimum phase $\{A(k)\}$ and maximum phase $\{B(k)\}$ parameters are given by,

$$g_x(k, 0, 0) = \begin{cases} -\frac{1}{k} \cdot A(k), & k = 1, \dots, p \\ \frac{1}{k} \cdot B(-k), & k = -1, \dots, -q \end{cases} \quad (3)$$

and $g_x(k, l, n)$ is the tricepstrum of the fourth order statistics $f_x(k, l, n)$ of the signal. In this paper the cepstrum coefficients in (2) are being used, for the detection problem given by (1) using the moments instead of the cumulants and we validate that using simulations in section 3 under the assumption 2 below. The following assumptions are being made.

- 1) Under H_0 it is assumed that $\{A(k)\}, \{B(k)\}$ for all k are identically to zero.
- 2) Under H_1 since the process $\{x(n)\}$ is not stationary, it is assumed availability of many data records, i.e., $x^{(i)}(n) = m(n) + w^{(i)}(n)$, $i = 1, \dots, M$ is the given ensemble data set, where $\{w^{(i)}(n)\}$ are different noise realizations of identical statistical properties then,

$$f_x(k, l, m) = E \left\{ \cdot \sum_n x(n)x(n+k)x(n+l)x(n+m) \right\} \quad (4)$$

- 3) Since $\{A(k)\}, \{B(k)\}$ are decaying sequences they can be truncated (2) and p, q finite integers can be used [15].

By choosing $p = q$ then (2) can be written,

$$\begin{aligned} c_x(m, n) &= \sum_{k=1}^p f_x(m, k, n) \cdot A(k, n) + \sum_{k=1}^p f'_x(m, k, n) \cdot B(k, n), \\ m &= -p, \dots, -1, 1, \dots, p \end{aligned} \quad (5)$$

where $\{A(k, n)\}, \{B(k, n)\}$, $f_x(m, k, n)$, $f'_x(m, k, n)$, denote the estimates of the corresponding values of (2) at time instant n based on N samples. In a matrix form,

$$\mathbf{F}(p, n) \cdot \mathbf{T}(p, n) = \mathbf{C}(p, n), \quad (6)$$

where the elements of $\mathbf{T}(p, n)$ are,

$$T(k, n) = \begin{cases} A(k, n), & k = 1, \dots, p \\ B(k-p, n), & k = p+1, \dots, 2p \end{cases} \quad (6.1)$$

and

$$\begin{aligned} \mathbf{F}(p, n) \\ = \left(\begin{array}{ccccc} f_x(p, 1, n) & \cdots & f_x(p, p, n) & f'_x(p, 1, n) & \cdots & f'_x(p, p, n) \\ \vdots & \ddots & \vdots & \vdots & \ddots & \vdots \\ f_x(-p, 1, n) & \cdots & f_x(-p, p, n) & f'_x(-p, 1, n) & \cdots & f'_x(-p, p, n) \end{array} \right), \end{aligned} \quad (6.2)$$

$$\mathbf{C}(p, n) = (c_x(p, n), \dots, c_x(-p, n))^T, \quad (6.3)$$

" T " denotes transpose operation.

It will be shown now that asymptotically under H_0 the matrix $\mathbf{F}(p, n)$ is of full, $2p$ rank. As $N \rightarrow \infty$ the only non-zero entries of the above matrix are the following,

$$f_x(m, m) = -\lim_{N \rightarrow \infty} \frac{1}{N} \cdot \sum_{n=0}^N x(n)^4, \quad (7.1)$$

$$f'_x(-m, m) = \lim_{N \rightarrow \infty} \frac{1}{N} \cdot \sum_{n=0}^N x(n)^4, \quad (7.2)$$

$$f_x(-m, m) = \lim_{N \rightarrow \infty} \frac{1}{N} \cdot \sum_{n=m}^N x(n)^2 x(n-m)^2, \quad (7.3)$$

$$f'_x(m, m) = -f_x(-m, m), \quad m = 1, \dots, p. \quad (7.4)$$

This means, the matrix $\mathbf{F}(p, n)$ is of full rank. Furthermore the solution from (6) does not depend on the variance of the noise which makes the detector of constant false alarm rate (CFAR). Thus, it is not necessary to estimate the variance of the noise in order to set the threshold as long as the data record is long enough so that the sample averages (7.1)–(7.3) give the true values.

Next it is shown that asymptotically under H_0 the estimates of the tricepstrum coefficients, $\{A(k)\}, \{B(k)\}$, are Gaussian random variables of zero mean and constant covariance matrix. Let $c_x(m, n) = m/N \sum_m^n x(n)x^3(n-m)$. Then (using the central limit theorem) the variables $c_x(m, n)$, $m = -p, \dots, -1, 1, \dots, p$ are zero mean with constant covariance matrix. It is also assumed that if $N \rightarrow \infty$ $f_x(m, k, n)$, $f'_x(m, k, n)$ become their true values $f_x(m, k)$, $f'_x(m, k)$. Then in the limit,

$$(A(1), \dots, A(p), B(1), \dots, B(p))^T \sim \mathbf{F}^{-1}(p) \cdot \mathbf{C}(p) \quad (8)$$

The covariance matrix of $\mathbf{T}(p, n)$ for $N \rightarrow \infty$ and for the case of additive white Gaussian noise (AWGN) is given by,

$$\Phi = \mathbf{F}^{-1}(p) \cdot E\{\mathbf{C}(p, N)\mathbf{C}^T(p, N)\}\mathbf{F}^{-T}(p), \quad (9)$$

where after the computations its elements are,

$$\Phi(i, j) = \begin{cases} a_i i^2, & i, j = 1, \dots, p \\ a_{i-p} \cdot (i-p)^2, & i, j = (p+1), \dots, 2p \\ b_i i^2, & i = 1, \dots, p, j = (p+1), \dots, 2p \\ b_j j^2, & i = (p+1), \dots, 2p, j = 1, \dots, p \end{cases}, \quad (10)$$

where $a_i = -150/(64(N-i))$, $b_i = -90/(64(N-i))$. Therefore, it can be used as a detection statistic the variable,

$$L_T = \sum_{k=1}^l (A(k, n)^2)/(\sigma_{a_k}^2) + (B(k, n)^2)/(\sigma_{b_k}^2), \quad (11)$$

where, $\sigma_{a_k}^2$, $\sigma_{b_k}^2$ are the variances of $A(k, n)$, $B(k, n)$. This is a central quadratic form ($l \leq p$).

Remarks.

1) Choosing appropriate combinations of the tricepstrum coefficients the detection variable L_T under H_0 becomes a central Chi-Square with $2l$ degrees of freedom (ex., $A(k), k = 1, \dots, p$).

2) The same decision variable can be used if the additive noise is non-Gaussian, i.i.d and non-skewed, where using (7.1)–(7.4) the elements of (10) will change appropriately.

3) For fixed probability of false alarm P_{FA} , the threshold can be computed using the cumulative distribution F_0 of L_T under H_0 ,

$$t_h = F_0^{-1}(1 - P_{FA}) \quad (12)$$

4) Instead of using fourth order statistics, third order statistics can be used. However, in this case the noise cannot be Gaussian, i.i.d. The additive white non-Gaussian noise (AWNGN) with zero mean assumption is enough to guarantee asymptotically under H_0 rank $2p$, for the matrix $\mathbf{F}(p)$.

Summarizing the algorithm for detecting deterministic transient signals embedded in additive white Gaussian noise we have the following:

1) Estimate the fourth order statistics of $f_x(k, l, n)$ [15].

2) Estimate $A(k)$, $B(k)$ using a least squares solution to the overdetermined system of equations (2) when $p = q, m = p, \dots, p-W$. $W \geq 2p$

3) Compute L_T and compare it with a threshold chosen according to (12).

2.2. The recursive approach

Instead of estimating the cepstrum coefficients $\{A(k)\}$ and $\{B(k)\}$ in one step when the whole data record is available we seek for a recursive solution of (6) which will allow for fast updating of the coefficients when new data arrive and the amount of the data is large. Another reason for developing a recursive approach is when the arrival times of the transients are unknown. It is assumed the following partition for $f_x(m, k, n)$, $f'_x(m, k, n)$.

$$\begin{aligned} f_x(m, k, n) &= \sum_{i=n_0+1}^n \lambda^{n-i} x(i) (x^2(i-m), 1) \\ &\quad \cdot (x(i-(m+k)), -x^3(i-(m+k)))^T \\ &\quad + \lambda^{n-n_0} f_x(m, k, n_0), \end{aligned} \quad (13.1)$$

$$\begin{aligned} f'_x(m, k, n) &= \sum_{i=n_0+1}^n \lambda^{n-i} x(i) (x^2(i-m), 1) \\ &\quad \cdot (-x(i-(m+k)), x^3(i-(m+k)))^T \\ &\quad + \lambda^{n-n_0} f'_x(m, k, n_0), \end{aligned} \quad (13.2)$$

where, λ is a weight constant, $0 < \lambda \leq 1$ and $f(m, k, n_0)$, $f'_x(m, k, n_0)$ are computed values from the initialization period which will be explained in the sequel. Also note that a time recursion for $C(p, n)$ is,

$$\mathbf{C}(p, n) = \lambda \cdot \mathbf{C}(p, n - 1) + \mathbf{a}^T(n), \quad (14)$$

$$\mathbf{a}(n) = (px^3(n-p)x(n), \dots, (-p)x^3(n+p)x(n)). \quad (15)$$

To realize this solution matrix $\mathbf{F}(p, n)$ is decomposed into two submatrices, \mathbf{V} and \mathbf{U} and their Q-R decomposition is updated at each time instant that new information is present, i.e.,

$$\mathbf{F}(p, n) = \mathbf{V}^T(p, n) \cdot \mathbf{U}(p, n), \quad (16.1)$$

$$V^T = \begin{bmatrix} x^2(n_0 + 1 - p)x(n_0 + 1) & \dots & \dots & \dots & \dots \\ \vdots & x^2(n_0)x(n_0 + 1) & \dots & \dots & \dots \\ \vdots & \vdots & x(n_0 + 1) & \dots & \dots \\ \vdots & \vdots & \vdots & x^2(n_0 + 2)x(n_0 + 1) & \dots \\ \vdots & \vdots & \vdots & \vdots & x(n_0 + 1) \\ \vdots & \vdots & \vdots & \vdots & \vdots \\ \vdots & \vdots & \vdots & \vdots & x^2(n_0 + 1 + p)x(n_0 + 1) \\ \vdots & \vdots & \vdots & \vdots & x(n_0 + 1) \\ x^2(n + 1 - p)x(n + 1) & \dots & \dots & \dots & \dots \\ \vdots & \vdots & \vdots & \dots & \dots \\ 0 & x^2(n)x(n + 1) & \dots & \dots & \dots \\ \vdots & \vdots & \vdots & \dots & \dots \\ 0 & \vdots & x(n + 1) & \dots & \dots \\ \vdots & \vdots & \vdots & x^2(n + 2)x(n + 1) & \dots \\ \vdots & \vdots & \vdots & \vdots & \dots \\ 0 & 0 & 0 & 0 & x^2(n + 1 + p)x(n + 1) \\ \vdots & \vdots & \vdots & \vdots & x(n + 1) \end{bmatrix} \quad (16.2)$$

which is $2px(2(n - n_0) + 4p)$

$$\mathbf{U} = \begin{bmatrix} x(n_0 - p) & \dots & x(n_0 - 2p + 1) & -x(n_0 - p + 2) & \dots & -x(n_0 + 1) \\ -x^3(n_0 - p + 2) & \dots & -x^3(n_0 + 1) & x^3(n_0 - p) & \dots & x^3(n_0 - 2p + 1) \\ x(n_0 - p + 1) & \dots & x(n_0 - 2p) & -x^3(n_0 - p + 3) & \dots & -x^3(n_0 + 2) \\ -x(n_0 - p + 3) & \dots & -x(n_0 + 2) & x^3(n_0 - p + 1) & \dots & x^3(n_0 - 2p + 2) \\ \vdots & \ddots & \vdots & \vdots & \ddots & \vdots \\ x(n - p - 1) & \dots & x(n - 2p) & -x(n - p + 1) & \dots & -x(n) \\ -x^3(n - p + 1) & \dots & -x^3(n) & x^3(n - p - 1) & \dots & x^3(n - 2p) \\ \vdots & \ddots & \vdots & \vdots & \ddots & \vdots \\ x(n + p - 1) & \dots & x(n) & -x(n + p + 1) & \dots & -x(n + 2p) \\ -x^3(n + p + 1) & \dots & -x^3(n + 2p) & x^3(n + p - 1) & \dots & x^3(n) \end{bmatrix} \quad (16.3)$$

which is $(2(n - n_0) + 4p)x2p$

To initialize the decomposition at time instant n_0 , $4p + 1$ samples are assumed to be available then, the initial \mathbf{V} and \mathbf{U} are,

$$V^T = \begin{bmatrix} 0 & . & . & . & . & . & 0 \\ x(0) & . & . & . & . & . & . \\ 0 & . & . & . & . & . & . \\ x(1) & . & . & . & . & . & . \\ 0 & . & . & . & . & . & . \\ . & . & . & . & . & . & . \\ 0 & . & 0 & . & . & . & . \\ x(p-1) & . & x(0) & . & . & . & . \\ x^2(0)x(p) & . & x^2(0)x(1) & 0 & . & . & . \\ x(p) & . & x(1) & 0 & . & . & . \\ x^2(1)x(p+1) & . & x^2(1)x(2) & x^2(1)x(0) & . & . & . \\ x(p+1) & . & x(2) & x(0) & . & . & 0 \\ x^2(p)x(2p) & . & x^2(p)x(p+1) & x^2(p)x(p-1) & . & x^2(p)x(0) \\ x(2p) & . & x(p+1) & x(p-1) & . & x(0) \\ 0 & . & . & . & . & x^2(p+1)x(1) \\ . & . & . & . & . & x(1) \\ . & . & 0 & x^2(2p-1)x(2p) & x(2p-1)x(p-1) \\ . & . & . & x(2p) & x(p-1) \\ . & . & . & . & . & x^2(3p)x(2p) \\ 0 & . & . & 0 & . & x(2p) \end{bmatrix} \quad (17.1)$$

which is $(2p)x(8p + 2)$ and (17.1)

$$\mathbf{U} = \begin{bmatrix} 0 & 0 & 0 & 0 & 0 & \dots & -x(0) \\ 0 & 0 & -x^3(0) & \cdot & \cdot & \cdot & 0 \\ \cdot & \cdot & \cdot & \cdot & \cdot & \cdot & \cdot \\ \cdot & \cdot & \cdot & \cdot & \cdot & \cdot & \cdot \\ 0 & 0 & 0 & 0 & -x(0) & -x(1) & -x(p-1) \\ -x^3(0) & -x^3(-1) & -x^3(p-1) & 0 & 0 & 0 & 0 \\ \cdot & \cdot & \cdot & \cdot & \cdot & \cdot & \cdot \\ x(p-2) & x(p-3) & 0 & -x(p) & -x(p+1) & -x(2p-1) \\ -x^3(p) & -x^3(p+1) & -x^3(2p-1) & x^3(p-2) & x^3(p-3) & \cdot & 0 \\ x(p-1) & x(p-2) & x(0) & -x(p+1) & -x(p+2) & \cdot & -x(2p) \\ -x^3(p+1) & -x^3(p+2) & -x^3(2p) & x^3(p-1) & x^3(p-2) & \cdot & x(0) \\ x(p) & x(p-1) & x(1) & -x(p+2) & -x(p+3) & \cdot & -x(2p+1) \\ -x^3(p+2) & -x^3(p+3) & -x^3(2p+1) & x^3(p) & x^3(p-1) & \cdot & x(1) \\ \cdot & \cdot & \cdot & \cdot & \cdot & \cdot & \cdot \\ x(3p-1) & x(3p-2) & x(2p) & -x(3p+1) & -x(3p+2) & \cdot & -x(4p) \\ -x^3(3p+1) & -x^3(3p+2) & -x^3(4p) & x^3(3p-1) & x^3(3p-2) & \cdot & x^3(2p) \end{bmatrix} \quad (17.2)$$

which is $(8p + 2)x(2p)$.

Both \mathbf{V}^T and \mathbf{U} start with,

$$\mathbf{Q}(1) \cdot \hat{\mathbf{A}}(1) = \begin{pmatrix} \mathbf{F}(1) \\ 0 \end{pmatrix}, \quad (18)$$

where, $\hat{\mathbf{A}}$ matrix will represent either \mathbf{V}^T or \mathbf{U} , $\mathbf{F}(1) = \mathbf{x}(0)$ and

$$\mathbf{Q}(1) = \begin{pmatrix} 0 & 1 \\ 0 & 0 \end{pmatrix}, \quad \hat{\mathbf{A}}(1) = \begin{pmatrix} 0 \\ x(0) \end{pmatrix}. \quad (19)$$

Given the above initial values, new data at each iteration i , for both \mathbf{V}^T and \mathbf{U} , namely $\mathbf{u}_{in1}(i)$ and $\mathbf{u}_{in2}(i)$ are obtained. The general notation $\mathbf{u}_{in}(i)$ is used here and the details are given in Table 1. Then Q-R decomposition is applied on, $\hat{\mathbf{A}}(1)$,

$$\hat{\mathbf{A}}(2) = \begin{pmatrix} \hat{\mathbf{A}}(1) & \mathbf{0}_{(2 \times 1)} \\ \mathbf{u}_{in}(i) \end{pmatrix}. \quad (20)$$

In the subsequent steps of the initialization period we input new data until we finally obtain Q-R decompositions for \mathbf{V}^T and \mathbf{U} .

It remains to describe the orthogonal transformations that are used to compute the Givens rotation parameters and then the Givens transformation matrix $G(i)$. In particular for each step, the partially triangularized matrix is assumed,

$$\mathbf{F}(i) = \begin{pmatrix} \mathbf{D}_{ixj}^{1/2}(i) \cdot \hat{\mathbf{F}}_{jxj}(i) \\ \mathbf{0}_{1 \times j} \end{pmatrix}, \quad (21.1)$$

$$j = \begin{cases} i, & i \leq 2p \\ 2p, & i > 2p \end{cases}, \quad (21.2)$$

where $\mathbf{D}^{1/2}(i)$ is diagonal matrix and $\hat{\mathbf{F}}(i)$ is a unit upper triangular matrix. The requirement is to find rotation parameters so that we can annihilate the new input vector $\mathbf{u}_{in}(i)$. Thus, a sequence of Givens rotations [25] is used, described by,

$$G_m(i, k, l) = \begin{cases} c_m(i), & k = l = m \\ s_m(i), & k = i, l = i + 1 \\ -s_m(i), & k = i + 1, l = m \\ c_m(i), & k = l = i + 1 \\ 1, & k = l, k \neq m, 1 \leq k < i \end{cases} \quad (22)$$

and the Givens transformation matrix itself is.

$$\mathbf{G}(i) = \prod_{m=1}^{l_n} G_m(i) \quad (23)$$

$$l_n = \begin{cases} k_n + 1, & k_n < 2p \\ 2p, & k_n = 2p \end{cases} \quad (23.1)$$

Table 1
Initialization of the tricepstrum recursions.

Based on minimum, $4p + 1$ sample obtain initial Q-R decompositions for

$$\mathbf{U}_{(8p+2)\times(2p)}(p, n_0), \quad \mathbf{V}_{(2p)\times(8p+2)}^T(p, n_0)$$

$$\mathbf{Q}_{jxj}^{(k)}(p, n_0) \cdot \hat{\mathbf{A}}_{jx2p}^{(k)}(p, n_0) = \begin{pmatrix} \mathbf{F}_{2px2p}^{(k)}(p, n_0) \\ \mathbf{0}_{(j-2p)\times(2p)} \end{pmatrix}$$

$$\mathbf{F}_{2px2p}^{(k)}(p, n_0) = \mathbf{D}_{2px2p}^{(k)1/2}(p, n_0) \cdot \hat{\mathbf{F}}_{2px2p}^{(k)}(p, n_0), \quad k = u, v$$

$$\hat{\mathbf{A}}^{(u)}(p, n_0) = \mathbf{U}_{(8p+2)\times(2p)}(p, n_0)$$

$$\hat{\mathbf{A}}^{(v)}(p, n_0) = \mathbf{V}_{(2p)\times(8p+2)}^T(p, n_0)$$

Input data for $\mathbf{V}^T(p, n_0)$ and $\mathbf{U}(p, n_0)$,

$$\mathbf{u}_{in}(i) = \begin{cases} (\sigma, \dots, \sigma)_{1\times 2p}, i \leq 2p \\ \mathbf{u}_{in1}(i) = (0, \dots, 0)_{1\times 2p}, \\ \mathbf{u}_{in2}(i) = (x(i - (2p + 1)), \dots, x(0), 0, \dots, 0)_{1\times 2p}, & 2p < i \leq 3p \\ \mathbf{u}_{in1}(i) = x^2(i - (3p + 1)) \cdot \mathbf{u}_{in2}(i), \\ \mathbf{u}_{in2}(i) = (x(i - (2p + 1)), \dots, x(0), 0, \dots, 0)_{1\times 2p}, & 3p + 1 \leq i \leq 4p + 1 \\ \mathbf{u}_{in1}(i) = x^2(i - (3p + 1)) \cdot \mathbf{u}_{in2}(i), \\ \mathbf{u}_{in2}(i) = (0, \dots, 0, x(2p), \dots, x(i - (2(2p) + 1)))_{1\times 2p}, & 4p + 2 \leq i \leq 6p + 1 \\ \mathbf{u}_{in2}(i) = (0, \dots, 0, x(2p), \dots, x(i - (2(2p) + 1)))_{1\times 2p}, & 6p + 2 \leq i \leq 8p + 1 \end{cases}$$

$$\mathbf{u}_{in}(i) = \begin{cases} (\sigma, \dots, \sigma)_{1\times 2p}, \quad i \leq 2 \\ \underbrace{(\sigma, \dots, \sigma, -x(0))_p, \sigma, \dots, \sigma}_{i-1} \mathbf{u}_{in1}(i) = (0, \dots, 0, 0, \dots, 0, -x(0), \dots, -x(i - (2p + 1)))_{1\times 2p} \\ \mathbf{u}_{in2}(i) = (0, \dots, 0, -x^3(0), \dots, -x^3(i - (2p + 1)), 0, \dots, 0)_{1\times 2p} & 3 \leq i \leq 2p \\ 2p + 1 \leq i \leq 3p + 1 \\ \mathbf{u}_{in1}(i) = (x(i - (3p + 2)), \dots, x(i - (4p + 1)), -x(i - 3p), \dots, -x(i - (2p + 1)))_{1\times 2p} \\ \mathbf{u}_{in2}(i) = (-x^3(i - 3p), \dots, -x^3(i - (2p + 1)), x^3(i - (3p + 2)), \dots, x^3(i - (4p + 1)))_{1\times 2p} & 3p + 2 \leq i \leq 6p + 1, x(j) = 0, j < 0 \end{cases}$$

where σ small constant.

where k_n is the dimension of the input vector. The recursive relationships for the rotation parameters are summarized in Table 2.

After the end of the initialization period initial Q-R decompositions for $\mathbf{V}^T(p, n)$ and $\mathbf{U}(p, n)$ are available. It is denoted again in general each one of them by $\hat{\mathbf{A}}(p, n)$. For $\mathbf{U}(p, n)$ the new data sets for the next iteration are the last two lines of (16.3), i.e., per iteration its Q-R decomposition is updated twice. For $\mathbf{V}^T(p, n)$, per iteration its Q-R decomposition is updated $4p + 2$ times, using equal number of new data sets, $\mathbf{u}_{in}(n, i)$, which are described as follows,

$$\mathbf{u}_{in}(n, i) = \begin{cases} \mathbf{u}_{in1}(n, i) = x(n - p + i) \cdot \mathbf{u}_{in2}(n, i), \\ \mathbf{u}_{in2}(n, i) \\ = (\underbrace{0, \dots, 0}_{i-1}, x(n + 1), \dots, x(n - (2p - i))), \\ i = 1, \dots, 2p + 1 \end{cases} \quad (24)$$

where the step $i = p + 1$ (which corresponds to $m = 0$, row of $\mathbf{F}(p, n)$ in (6)) is ignored. The decomposition of the first step $i = 1$ is stored for each time instant n and is used as initial for the iterations, $i = 1, \dots, 2p + 1$ of the next time instant $n + 1$ for $\mathbf{V}^T(p, n)$.

I.e., summarizing the update process for both $\mathbf{V}^T(p, n)$, $\mathbf{U}(p, n)$ for every time instant n we have the following,

$$\mathbf{Q}_{jxj}(p, n) \cdot \hat{\mathbf{A}}_{jx2p}(p, n) = \begin{pmatrix} \mathbf{F}_{2px2p}(p, n) \\ \mathbf{0}_{(j-2p)\times 2p} \end{pmatrix}, \quad (25.1)$$

$$\mathbf{F}_{2px2p}(p, n) = \mathbf{D}_{2px2p}^{(k)1/2}(p, n) \cdot \hat{\mathbf{F}}_{2px2p}(p, n), \quad (25.2)$$

where $j = 2(n - n_0) + 8p + 2$ for $\mathbf{U}(p, n)$ and $j = 2(n - n_0) + 4p + 2$ for $\mathbf{V}^T(p, n)$ and it was assumed that $n_0 = 2p$. At the next time instant $n + 1$, new information is available (note that at time instant n , samples of a growing rectangular window are available up to time instant $n + 2p$, i.e., when it is said new available information it is meant that this window is moved one position forward) and $\hat{\mathbf{A}}(p, n)$ and $\mathbf{F}(p, n)$ matrices are updated,

$$\hat{\mathbf{A}}(p, n + 1, i) = \begin{pmatrix} \hat{\mathbf{A}}(p, n, i) \\ \mathbf{u}_{in}(n, i) \end{pmatrix}, \quad (26.1)$$

$$\mathbf{F}^*(n + 1, i) = \begin{pmatrix} \mathbf{F}_{2px2p}(p, n, i) \\ \mathbf{0}_{(j-2p)\times 2p} \\ \mathbf{u}_{in}(n, i) \end{pmatrix}, \quad (26.2)$$

Table 2
Recursions for Givens rotations parameters.

$$f_{ik}(m, k, n), i = 1, \dots, 2p, k = 1, \dots, 2p$$

elements of an upper triangular matrix

$$d_i^{1/2}(m, k, n) = f_{ii}(m, k, n), \quad i = 1, \dots, 2p$$

$$\hat{r}_{ik}(m, k, n) = \frac{f_{ik}(m, k, n)}{d_i^{1/2}(m, k, n)}, \quad i, k = 1, \dots, 2p$$

Do $i = 1, \dots, j$

$$d_i(n) = d_i(n-1) + \delta_{i-1}(n)[u_i^{(i-1)}(n)]^2, \quad u_i^{(0)} = u_i, \quad \delta_0(n) = 1.$$

$$\hat{s}_i(n) = \frac{\delta_{i-1}(n)}{d_i(n)} u_i^{(i-1)}(n)$$

$$s_i(n) = \frac{d_i^{1/2}(n)}{\delta_{i-1}^{1/2}(n)} \hat{s}_i(n)$$

$$\hat{c}_i(n) = \frac{d_i(n-1)}{d_i(n)}$$

$$c_i(n) = \frac{d_i^{1/2}(n)}{d_i^{1/2}(n-1)} \hat{c}_i(n)$$

$$\hat{r}_{ik}(n) = \hat{c}_i(n) \hat{r}_{ik}(n-1) + \hat{s}_i(n) u_k^{(i-1)}(n), \quad k = i+1, \dots, j$$

$$\delta_i(n) = \frac{d_i(n-1)}{d_i(n)} \delta_{i-1}(n)$$

$$u_k^{(i)}(n) = u_k^{(i-1)}(n) - u_i^{(i-1)}(n) \hat{r}_{ik}(n-1), \quad k = i+1, \dots, j$$

End do

Givens Transformation matrix $\mathbf{G}(n)$

$$\mathbf{G}(n) = \prod_{m=1}^{l_n} G_m(n)$$

$$G_m(n, i, j) = \begin{cases} c_m(n)i = j = m \\ s_m(n)i = m, \quad j = n+1 \\ -s_m(n)i = n+1, \quad j = m \\ c_m(n)i = j = n+1 \\ 1, \quad i = j, i \neq m, 1 \leq i < n \end{cases}$$

$$l_n = \begin{cases} k_n + 1 \quad k_n < 2p \\ 2p \quad k_n - 2p \end{cases}$$

the index i is used here to indicate the iterations for every time instant n . Note that, $\hat{\mathbf{A}}(p, n) = \hat{\mathbf{A}}(p, n, 1)$ and $\mathbf{F}(p, n) = \mathbf{F}(p, n, 1)$ also for $\mathbf{U}(p, n), i = 1$, where as for $\mathbf{V}^T(p, n), i = 1, \dots, 2p+1$.

Using the recursions summarized in Table 2 the rotation parameters are computed and the sequence of the square root Givens rotations are applied at time instant n on $\mathbf{F}(p, n)$ to annihilate all $2p$ elements of the last row. Tables 1–3 summarize the recursions. Then,

$$\mathbf{G}(n+1, i) \cdot \mathbf{F}_{(j+1)\mathbf{x}2\mathbf{p}}^*(n+1, i) = \begin{pmatrix} \mathbf{F}_{2\mathbf{p}\mathbf{x}2\mathbf{p}}(p, n, i) \\ \mathbf{0}_{(j+1-2p)\mathbf{x}(2p)} \end{pmatrix}, \quad (27.1)$$

$$\mathbf{Q}_{(j+1)\mathbf{x}(j+1)}(p, n+1, i) = \mathbf{G}(n+1, i) \cdot \begin{pmatrix} \mathbf{Q}_{j\mathbf{x}j}(p, n, i) & \mathbf{0}_{j\mathbf{x}1} \\ \mathbf{0}_{1\mathbf{x}j} & 1 \end{pmatrix}, \quad (27.2)$$

which gives the following Q-R decomposition at time instant $n+1$,

$$\hat{\mathbf{A}}_{j\mathbf{x}2\mathbf{p}}(p, n+1) = \mathbf{Q}_{j\mathbf{x}j}^T(p, n+1) \cdot \begin{pmatrix} \mathbf{F}_{2\mathbf{p}\mathbf{x}2\mathbf{p}}(p, n+1) \\ \mathbf{0}_{(j-2p)\mathbf{x}(2p)} \end{pmatrix}, \quad (28)$$

where now $j = 2(n+1-n_0)+8p+2$ for both $\mathbf{V}^T(p, n)$, $\mathbf{U}(p, n)$. If indexes u, v are used to denote the corresponding \mathbf{Q} , \mathbf{F} matrices for $\mathbf{V}^T(p, n)$, $\mathbf{U}(p, n)$ then the least squares solution (6) can be realized as,

$$\mathbf{F}^{(u)} \cdot \mathbf{T} = (\mathbf{Q}^{(v)}(\mathbf{Q}^{(u)})^T)^{-1} \cdot (\mathbf{F}^{(v)})^{-T} \cdot \mathbf{C}, \quad (29.1)$$

where, $\mathbf{F}^{(u)}$, $\mathbf{F}^{(v)}$ are $2px2p$, $\mathbf{Q}^{(v)}$ is $(2pxj)$ and $\mathbf{Q}^{(u)}$ is $(2pxj)$ and $j = 2(n+1-n_0)+8p+2$. The two square matrices on the right hand side of (29.1) are invertible because of the way that they were constructed using the Givens rotations and the above linear system of equations can be solved using back substitution. An attempt to use symmetric matrices to realize a least squares solution for (6) gives,

$$\mathbf{T}(p, n) = (\mathbf{F}^T(p, n)\mathbf{F}(p, n))^{-1} \cdot \mathbf{F}^T(p, n)\mathbf{C}(p, n), \quad (29.2)$$

where, because of the assumed Q-R decomposition of the data matrices we have the following equivalent form to (29.2),

$$\mathbf{T} = (\mathbf{R}^{(v)}\mathbf{R}^{(u)})^T \cdot (\mathbf{R}^{(v)}\mathbf{R}^{(u)})^{-1} \cdot (\mathbf{R}^{(v)}\mathbf{R}^{(u)})^T \cdot \mathbf{C}, \quad (29.3)$$

where $\mathbf{R}^{(k)}, k = u, v$ is $\mathbf{Q}^{(u)}\mathbf{F}^{(u)}$, or $\mathbf{F}^{(v)}\mathbf{Q}^{(v)}$ (the indexes, p, n are dropped here and in (29.1)) and $\mathbf{F}^{(v)}$ is $(2px2p)$, $\mathbf{Q}^{(v)}$, $(2pxj)$, $\mathbf{F}^{(u)}$, $(2px2p)$, $\mathbf{Q}^{(u)}$, $(jx2p)$ and $j = 2(n+1-n_0)+8p+2$.

Under H_0 it was shown that asymptotically, $\mathbf{F}(p, n)$ is a full $2p$ rank matrix. Under H_1 despite of the fact that (2), does not fit the signal it has been demonstrated [26], that the cepstrum coefficients are useful in modeling the signal in the presence of AWGN. It was assumed however that (2) was truncated using $p = q$ finite integers. In Appendix B it is shown that if the signal is a superposition of damped sinusoids, i.e.,

$$m(n) = \sum_{i=1}^M h_i \cdot e^{b_i n}, \quad n = 0, 1, 2, \dots \quad (30)$$

where the complex constants are defined as

$$h_i \triangleq d_i e^{j\theta i}, \quad b_i \triangleq -c_i + j w_i, \quad c_i > 0 \quad (31)$$

then selecting, $2p \leq M$ a full rank $2p$ matrix is obtained, in the absence of noise. In the presence of noise when the recursive approach is used, it is essentially limited to one data record. When the fourth order statistics in (2) are estimated, since the process is non-stationary it is substituted the ensemble averages by time averages under the assumption that the process is locally stationary [27], i.e.,

$$f_x(k, l, m) = (1/N) \sum_n x(n)(n+k)x(n+l)x(n+m), \quad k, l, m \ll N \quad (32)$$

The above assumption is not strong given that we want $2p \leq M$.

2.3. Computational complexity

Finally, it is noted that the number of operations (multiplications and additions per iteration, MADPR) for the proposed method is of order of magnitude proportional to the time index n . This is because of the nature of the Q-R decomposition. Assuming a standard overhead for matrix inversion using a Q-R decomposition

Table 3

Summary of the Triceptrum Q–R recursions.

Available at time n :

$$\mathbf{T}_{2px1}(p, n), \mathbf{D}_{2px2p}^{(k)}(p, n)$$

$$\mathbf{F}_{2px2p}^{(k)}(p, n), \mathbf{Q}_{jxj}^{(k)}(p, n), k = u, v$$

New Information:

$$x(n)$$

Time Update Recursions:

$$\mathbf{u}_{in}^{(u)}(n, i) = \begin{cases} (x(n+p-1), \dots, x(n), -x(n+p+1), \dots, -x(n+2p)), & i=1 \\ (-x^3(n+p+1), \dots, -x^3(n+2p), x^3(n+p-1), \dots, x^3(n)), & i=1 \end{cases}$$

$$\mathbf{u}_{in}^{(v)}(n, i) = \begin{cases} \mathbf{u}_{in1}(n, i) = x(n-p+i) \cdot \mathbf{u}_{in2}(n, i), \\ \mathbf{u}_{in2}(n, i) = (\overbrace{0, \dots, 0}^{i-1}, x(n+1), \dots, x(n-(2p-i))), \\ i=1, \dots, 2p+1 \end{cases}$$

$$\begin{pmatrix} \mathbf{F}_{2px2p}^{(k)}(p, n+1, i) \\ \mathbf{O}_{(j+i-(2p+1))x(2p)} \end{pmatrix} = \mathbf{G}^{(k)}(n+1, i) \cdot \begin{pmatrix} \mathbf{F}_{2px2p}^{(k)}(p, n, i) \\ \mathbf{O}_{(j-2p)x2p} \\ \mathbf{u}_{in}^{(k)}(n, i) \end{pmatrix}$$

$$\mathbf{F}_{2px2p}^{(k)}(p, n+1, i) = \mathbf{D}_{2px2p}^{(k)1/2}(p, n+1, i) \hat{\mathbf{F}}_{2px2p}^{(k)}(p, n+1, i)$$

$$\mathbf{Q}_{(j+i+1)x(j+i+1)}^{(k)}(p, n+1, i) = \mathbf{G}^{(k)}(n+1, i) \cdot \begin{pmatrix} \mathbf{Q}_{(j+i)x(j+i)}^{(k)}(p, n, i) & \mathbf{O}_{1x(j+i)} \\ \mathbf{O}_{(j+i)x1} & 1 \end{pmatrix}$$

$$i = \begin{cases} 1, & k=u \\ 1, \dots, 2p+1, & k=v \end{cases}$$

$$j = \begin{cases} 2(n-n_0) + 8p + 2, & k=u \\ 2(n-n_0) + 4p + 2, & k=v \end{cases}$$

$$\mathbf{F}_{2px2p}^{(u)} \cdot \mathbf{T} = [\mathbf{Q}_{2px1}^{(v)} \cdot (\mathbf{Q}^{(u)})_{lx2p}^T]^{-1} \cdot (\mathbf{F}_{2px2p}^{(v)})^{-T} \cdot \mathbf{C}$$

$$l = 2(n+1-n_0) + 8p + 2$$

equal to $16p^3(s^2 + 1)$ [28] (where s is the maximum number of iterations required to reduce a superdiagonal element to zero in the SVD routine in [28] and k is the equivalent number of operations for square-root operation) we count $9p^2n + (204 + 16s^2)p^3 + 8p^2 + (\frac{272}{6} + 8k)p + 4$, MADPR (ex., for $s \approx 2p$, $k \approx 2$, $p = 2$, we obtain $36n + 3839$, MADPR). The number of operations according to (29.3) is $(8p-1)4pm + (\frac{2128}{6} + 16s^2)p^3 + 72p^2 + (\frac{188}{6} + 8k+4)p + 4$, MADPR. In the next section the proposed recursive approach is compared with an adaptive algorithm based on modeling the signal as an infinite impulse response (IIR). Since this is a fast algorithm it requires much less number of operations per recursion (about $7p$, p is the order of the IIR model) and the price paid is much worse performance.

2.4. Detection analysis

The distribution of (11) under H_0 was discussed in section 2.1 Under H_1 , let us assume that the solution of (6) has the following form,

$$\mathbf{T}(p, n) = f(\mathbf{m} + \mathbf{w}), \quad (33)$$

where \mathbf{m} , \mathbf{w} are the signal and noise vectors of the observation data record, (1) and f is a continuous function. If Taylor Expansion of (33) is assumed around the signal vector then it is obtained [29],

$$\begin{aligned} T(k, n) &= f_k(\mathbf{m}) + \mathbf{F}'(\mathbf{x})^T \cdot \mathbf{w} + (1/2)\mathbf{w}^T \cdot \mathbf{F}''(\mathbf{x}) \cdot \mathbf{w} + \dots, \\ k &= 1, \dots, 2p \end{aligned} \quad (34)$$

Where it is being kept only the first three terms of the expansion and “” denotes here first and second derivatives of f evaluated in the signal vector \mathbf{m} . By invoking the central limit theorem since \mathbf{w} is white i.i.d. noise if n is large enough then $T(k, n)$, $k = 1, \dots, 2p$, are jointly Gaussian random variables and the mean and covariance matrix of $\mathbf{T}(p, n)$ can be computed using,

$$E\{\mathbf{T}(p, n)\} \simeq \mathbf{F}^{-1}(p, n) \cdot \bar{\mathbf{C}}(p, n), \quad (35)$$

$$\begin{aligned} \Phi(p, n) &\simeq \bar{\mathbf{F}}^{-1}(p, n) \cdot E\{\mathbf{C}(p, n)\mathbf{C}^T(p, n)\} \\ &\quad \cdot \bar{\mathbf{F}}^{-T}(p, n) - \bar{\mathbf{T}}(p, n)\bar{\mathbf{T}}^T(p, n), \end{aligned} \quad (36)$$

where “–” denotes mean. The characteristics function $S(w)$ of a quadratic form given by,

$$L_T = \mathbf{T}^T(p, n)\mathbf{B}\mathbf{T}(p, n) \quad (37)$$

where \mathbf{B} is known is [30],

$$\begin{aligned} S(w) &= \frac{1}{|\mathbf{I} - 2jw\Phi(p, n)\mathbf{B}|^{1/2}} \\ &\quad \cdot \exp(jw\bar{\mathbf{T}}^T(p, n)\mathbf{B}(\mathbf{I} - 2jw\Phi(p, n)\mathbf{B})^{-1}\bar{\mathbf{T}}(p, n)). \end{aligned} \quad (38)$$

where \mathbf{I} is the identity matrix. By inverse Fourier transforming $S(w)$, the cumulative distributions F_0 under H_0 and F_1 under H_1 are computed. Then computing the threshold according to (12) the probability of detection will be, $P_D = 1 - F_1(L_T < t_h)$.

3. Simulation examples

Five (5) different transient signals embedded in AWGN and AWNGN are considered in this section in order to demonstrate the performance of the tricepstrum based detector. In terms of probability of detection and probability of false alarm (P_{FA}) we compare the batch approach with the energy detector by means of Monte-Carlo simulations. The recursive approach is compared with an adaptive algorithm which is based on representing the transient as an all-pole infinite impulse response (IIR) model [31].

Test Case 1 (Mixed phase transients, known arrival time).

Batch implementation: The z -transforms of the infinite duration signals which are both mixed phase are given by, example 1,

$$F(z) = \frac{(1 - 0.1z)}{z^2 - (1.1399)z + 0.3679} \quad (39.1)$$

and example 2,

$$\begin{aligned} F(z) = & (z^{-2}(z^6 - (0.6844)z^5 - (0.772)z^4 + (1.5283)z^3 \\ & - (1.9387)z^2 + (1.3289)z - (0.3128))) \\ & /(z^2 - (1.3688)z + 0.5488)(z^2 - (1.1399)z + 0.3679). \end{aligned} \quad (39.2)$$

Both signals are assumed to be of known arrival time for the batch approach. The energy detector which represents a lower bound on the detection performance is given by,

$$d = (1/\sigma_w^2) \sum_{i=0}^{N-1} x^2(i) \quad (39.3)$$

and it requires knowledge of the noise variance. The SNR is given by the ratio of the total signal energy to the variance of the noise and the data size was taken to 16 records by 100 samples per record. The probability of detection as a function of SNR for fixed probabilities of false alarm $0.05, 10^{-2}, 10^{-3}$ for example 1 is shown in Fig. 1a for the energy detector and the tricepstrum based detector. For these results 200 trials were performed with $p = q = 2$, and $l = 1$. The experimental and theoretical distributions of the tricepstrum based detector under H_0 are given in Fig. 1b for 1000 Monte-Carlo runs. We observe that for this data size and $l = 1$ the two distributions are very close and the probabilities of false alarm can be estimated by the theoretical distribution of L_T under H_0 . For the second example and for the same p, q , the detection performance is shown in Fig. 1c. In this example 500 sample sequences were generated for the computation of the probability of detection. Finally in order to demonstrate the insensitivity of the detector when the signal is embedded in zero mean non-Gaussian, i.i.d., noise (AWNGN), we tested the signal of example 1 assuming uniform distribution for the noise. Figs. 2a, 2b show the performance in this case.

Test Case 2 (Minimum phase transient, unknown arrival time).

Adaptive Implementation: The z -transform of the minimum phase signal is described by, example 3,

$$F(z) = \frac{1}{z^2 - (1.35)z + 0.75} \quad (40)$$

and we assume that it is of unknown arrival time at 200 samples. The signal plus noise records for AWGN of variance, $\sigma_w^2 =$

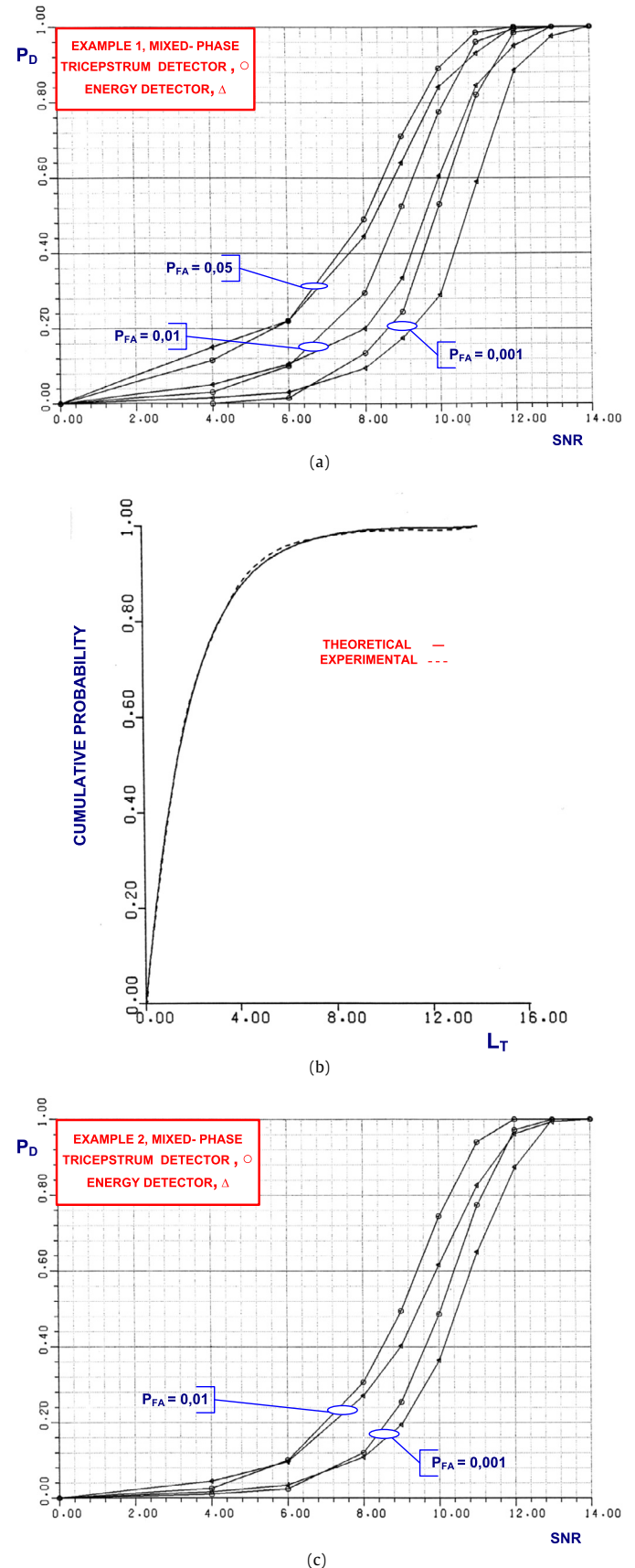


Fig. 1. Additive White Gaussian Noise: (a) probability of detection versus SNR for the signal of example 1, $P_{FA} = 0.05 \cdot 10^{-2}, 10^{-3}$, 16 records, 100 samples per record; (b) Cumulative distribution of L_T under H_0 for $p = q = 2$; (c) probability of detection versus SNR for example 2, $P_{FA} = 10^{-2}, 10^{-3}$, 16 records, 100 samples per record.

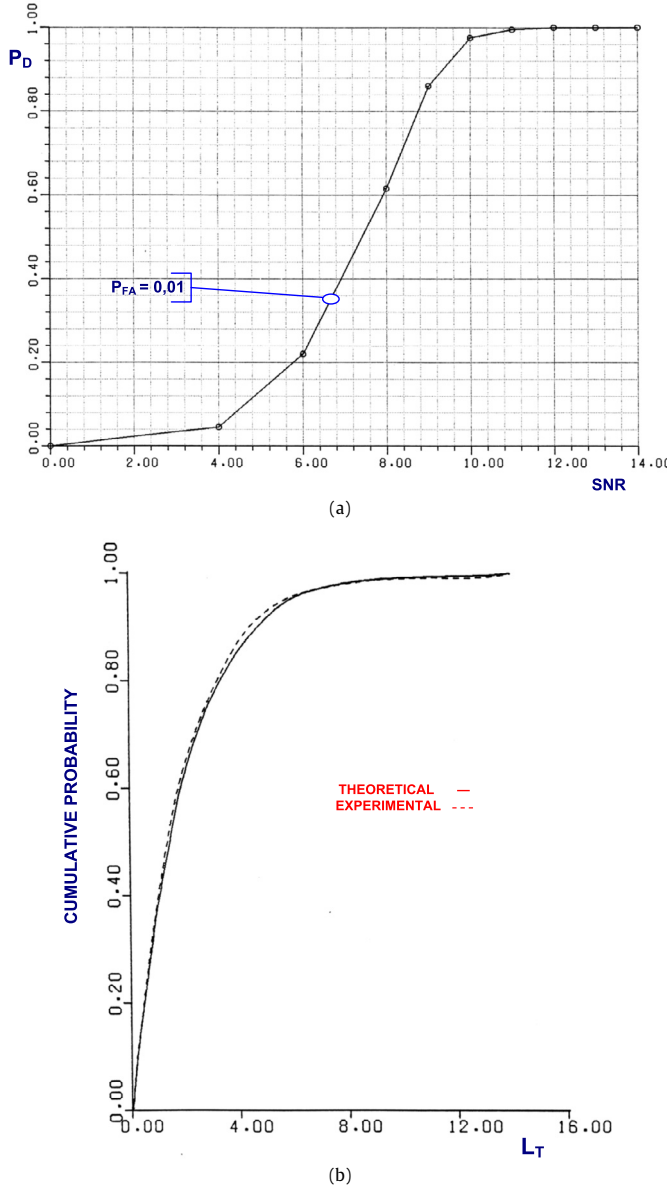


Fig. 2. Additive White non-Gaussian Noise, Uniform Distribution zero mean: (a) probability of detection versus SNR for example 1; (b) cumulative distribution of L_T under H_0 for $p = q = 2$.

3.162×10^{-1} , 0.1, for 15 sample signal are shown in Fig. 3a, 3b. In Fig. 4a, 4b we plot the detection statistics for the tricepstrum method and for the IIR adaptive algorithm versus time (the same way as for the definition of L_T , we use the sum of the squares of the estimated coefficients of the recursive IIR model as a detection statistic for the comparison algorithm). For the tricepstrum $p = q = 2$ and $l = 2$ and for the IIR model order, 2 were the choices for this experiment. For all the experiments below, including this one we keep l equal to the order of the model. Both methods under H_0 ($0, \dots, 199$) samples remain in the zero state and when the transient appears they jump and slowly converge again to the zero state. The weighting constant λ was for both methods 0.99. In Fig. 4c, we show operation of the algorithms for noise variance $\sigma_w^2 = 1$ and $\lambda = 0.98$.

Test Case 3 (Mixed phase transients, unknown arrival times).

Adaptive Implementation: The mixed phase transients are described by, example 4,

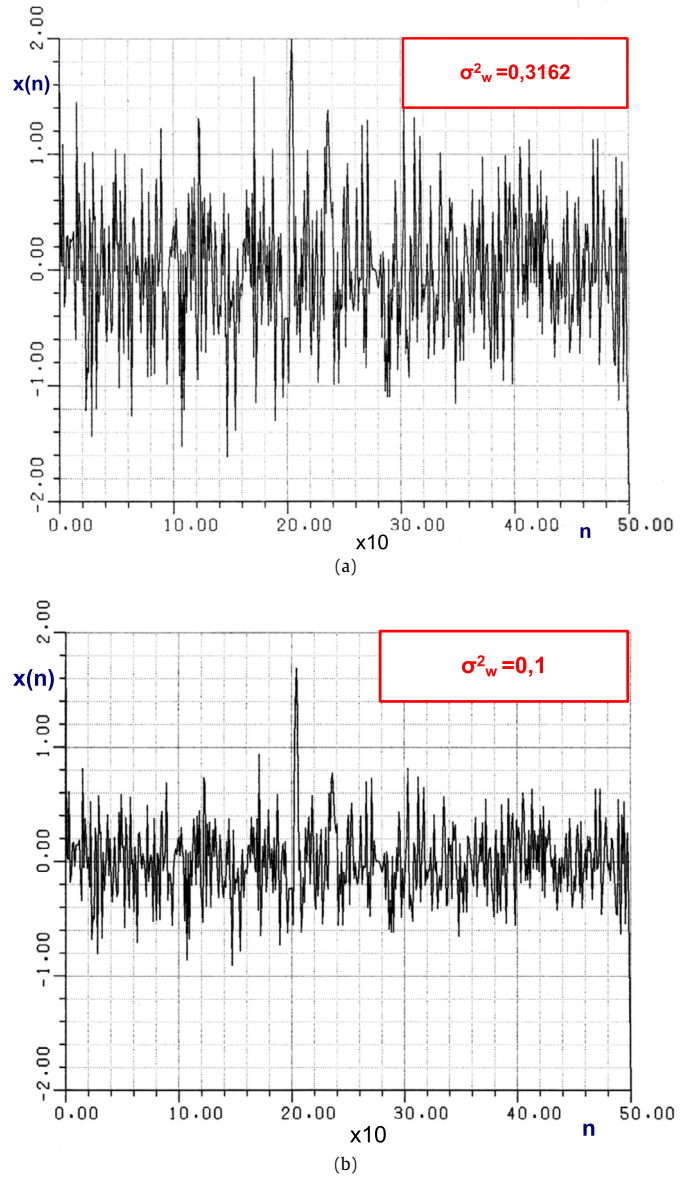


Fig. 3. Signal plus noise records for the minimum-phase signal, example 3, 15 samples, arrival time, 200 samples: (a) $\sigma_w^2 = 3.162 \times 10^{-1}$, (b) $\sigma_w^2 = 0.1$.

$$F(z) = \frac{(1 - 0.5z)(z^2 - (1.09754)z + (0.3012))}{z^2 - (0.6098)z + 0.3012} \quad (41.1)$$

example 5,

$$F(z) = \frac{(1 - 0.5z)(1 - 0.2z)(z^4 - (2.1481)z^3 + (1.8221)z^2 - (0.7202)z + 0.1108)}{z^4 - (1.7092)z^3 + (1.3395)z^2 - (0.5555)z + 0.1108} \quad (41.2)$$

For example 4, we use 15 sample signal and arrival time at 150 samples. The tricepstrum and IIR detection statistics versus time are shown in Figs. 5a, 5b. The noise variance is $\sigma_w^2 = 0.1, 3.162 \times 10^{-2}$ and we choose $p = 2$ for the tricepstrum and order 6 for the IIR, $\lambda = 0.99$ for both. It is clear that because of the inability of the IIR model to catch the non-minimum phase character of the signal its performance becomes much worse. This becomes more apparent if we compare Figs. 5a and 5b, where the SNR values are 13.8 dB and 12 dB correspondingly. In example 5, we make the non-minimum phase character of the signal

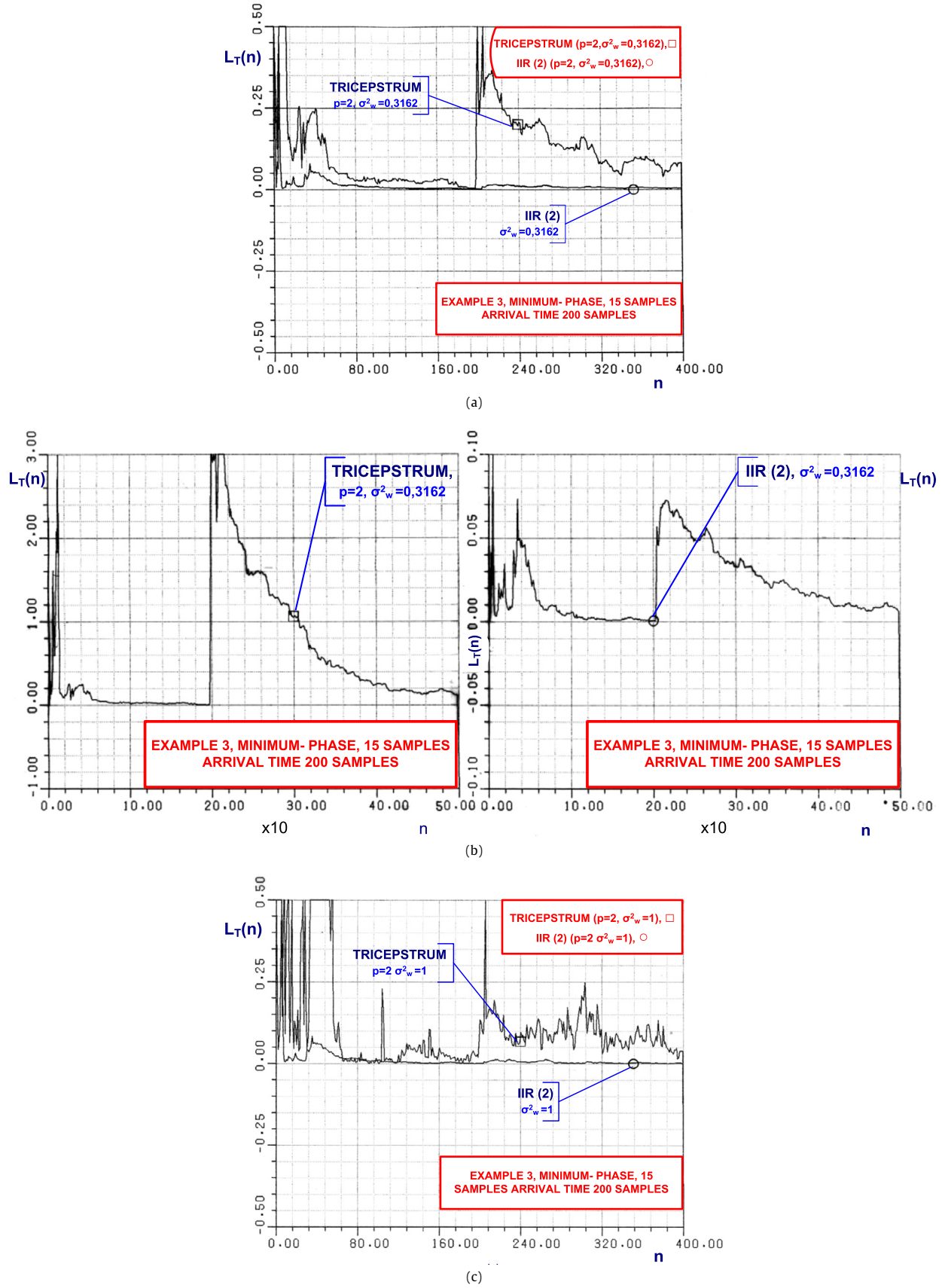
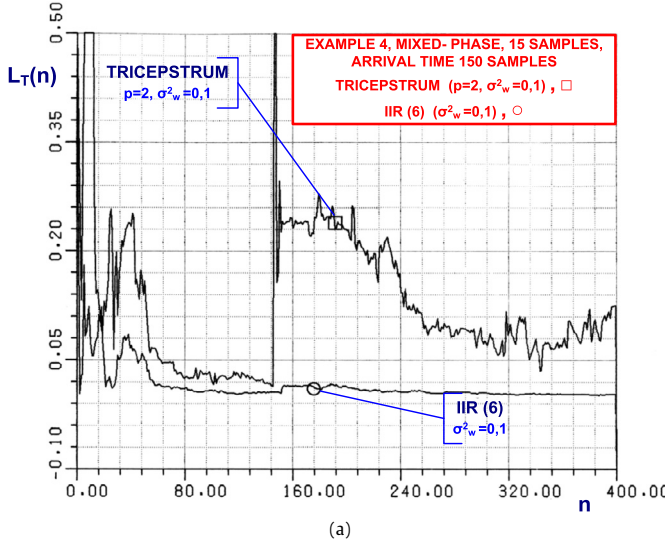
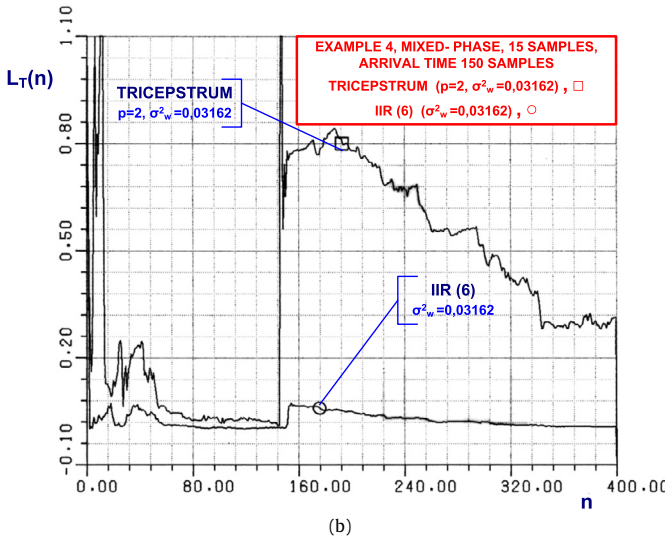


Fig. 4. Additive White Gaussian Noise, minimum-phase signal, example 3, 15 samples, arrival time, 200 samples, L_T versus time $\lambda = 0.99$, (a) Tricepstrum, $p = 2$ and IIR(2), $\sigma_w^2 = 3.162 \times 10^{-1}$, (b) $\sigma_w^2 = 0.1$, (c) $\sigma_w^2 = 1$, $\lambda = 0.98$.



(a)



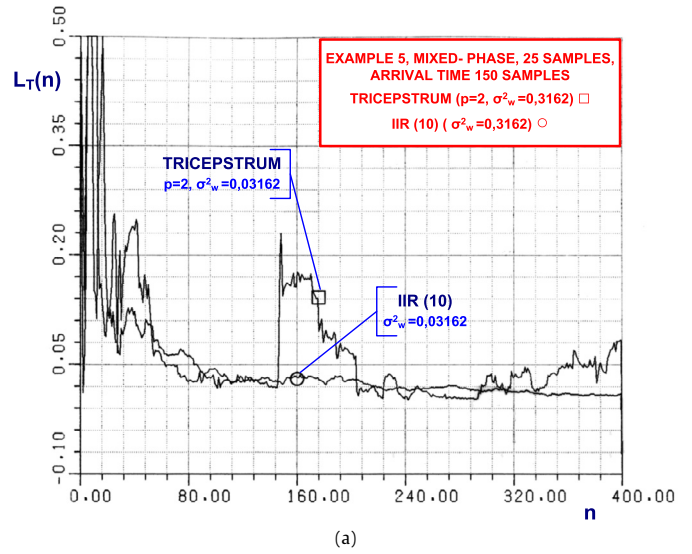
(b)

Fig. 5. Additive White Gaussian Noise, mixed-phase signal, example 4, 15 samples, arrival time, 150 samples: (a) L_T versus time, $\lambda = 0.99$, Tricepstrum, $p = 2$ and IIR(6), $\sigma_w^2 = 0.1$, (b) L_T versus time, $\lambda = 0.99$, $\sigma_w^2 = 3.162 \times 10^{-2}$.

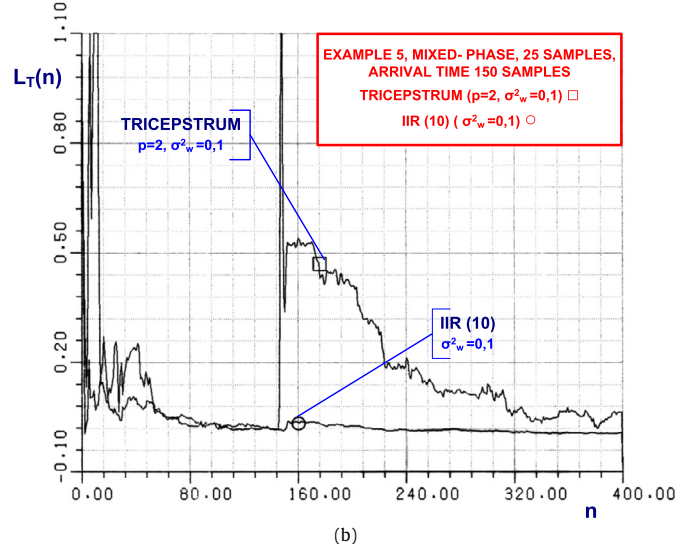
even stronger and we plot also the detection statistics for both methods in Figs. 6a–6c, for 25 sample signal and corresponding noise variances, $\sigma_w^2 = 3.162 \times 10^{-1}, 0.1, 3.162 \times 10^{-2}, 10^{-2}$. The orders of the tricepstrum and IIR methods were 2 and 10 with $\lambda = 0.99$. The performance of the first improves and for the second becomes worse with respect to examples 4 and 3. In Fig. 7 we plot for $p = 3$, $\lambda = 0.99$ and $\sigma_w^2 = 3.162 \times 10^{-2}, 0.1$ the tricepstrum detection statistic for examples 4, 5 to demonstrate performance with increased order. Note that varying the order of the IIR method does not change the situation shown in Figs. 4–6.

Test Case 4 (Two transients of unknown arrival time).

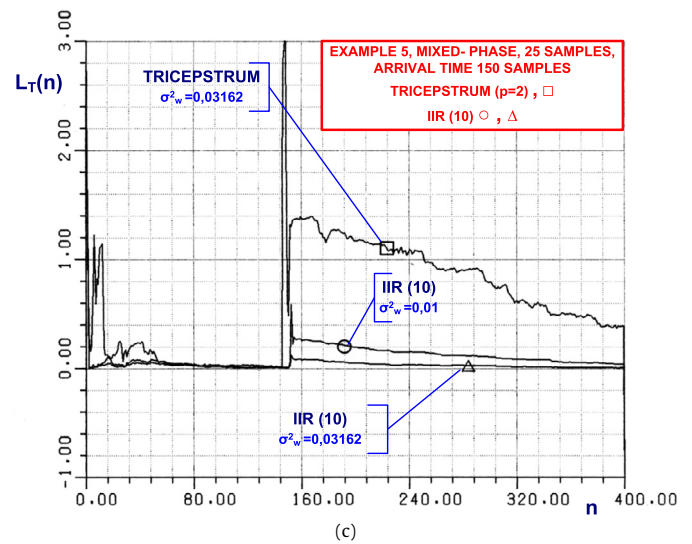
Adaptive Implementation: We let in this case two transients within the same data record. First we insert the mixed-phase signal of example 4, at 150 samples and the minimum-phase signal of example 3, at 350 samples. The signal lengths are 15 and 25. In Fig. 8a, we show relative performance of both methods, where for the tricepstrum the noise variance is $\sigma_w^2 = 0.1$, $p = 2$, $\lambda = 0.99$ and for the IIR method we use $\sigma_w^2 = 0.1, 3.162 \times 10^{-2}$, order 10, $\lambda = 0.99$. The difference in performance is clear and also the inability of the second method to detect the mixed-phase signal even



(a)

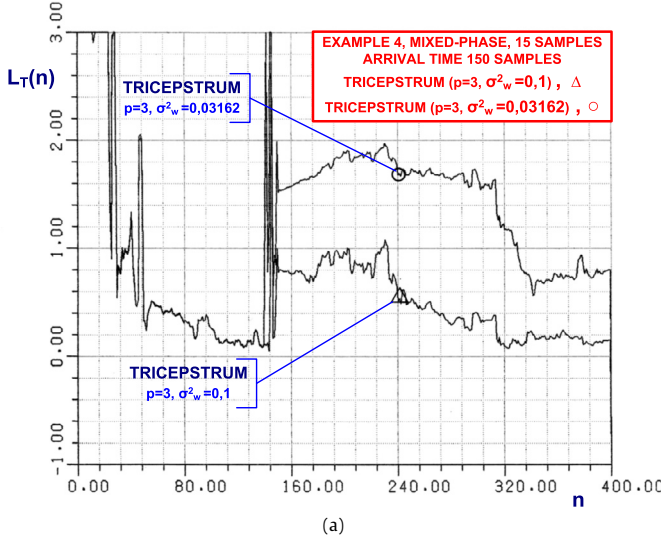


(b)

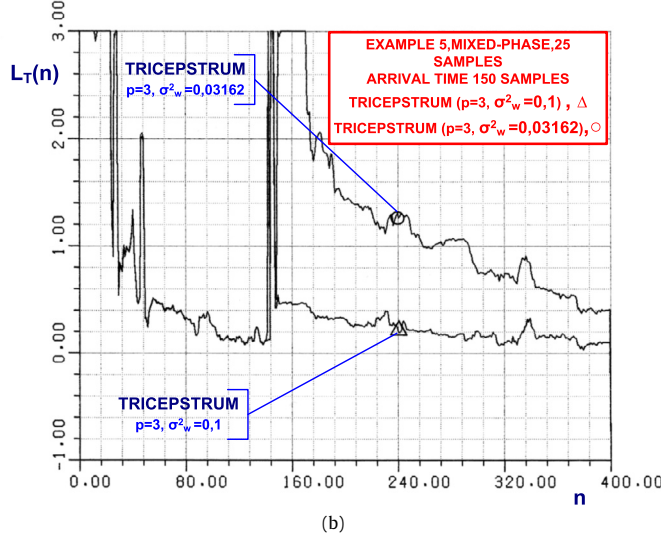


(c)

Fig. 6. Additive White Gaussian Noise, mixed-phase signal, example 5, 25 samples, arrival time 150 samples: (a) L_T versus time, $\lambda = 0.99$, Tricepstrum, $p = 2$ and IIR(10), $\sigma_w^2 = 3.162 \times 10^{-1}$, (b) L_T versus time, $\lambda = 0.99$, $\sigma_w^2 = 0.1$, (c) L_T versus time, $\lambda = 0.99$, $\sigma_w^2 = 3.162 \times 10^{-2}, 10^{-2}$ for IIR(10) and $\sigma_w^2 = 3.162 \times 10^{-2}$ for tricepstrum.



(a)



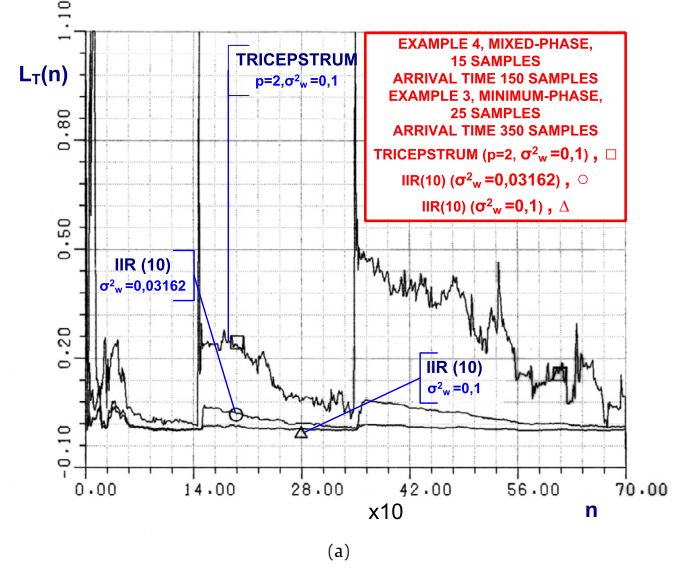
(b)

Fig. 7. Additive White Gaussian Noise, mixed-phase signals, examples 4, 5, 15, 25 samples, arrival time 150 samples, L_T versus time, $\sigma_w^2 = 0.1, 3.162 \times 10^{-2}$, Tricepstrum $p = 3$, $\lambda = 0.99$, (a) example 4, (b) example 5.

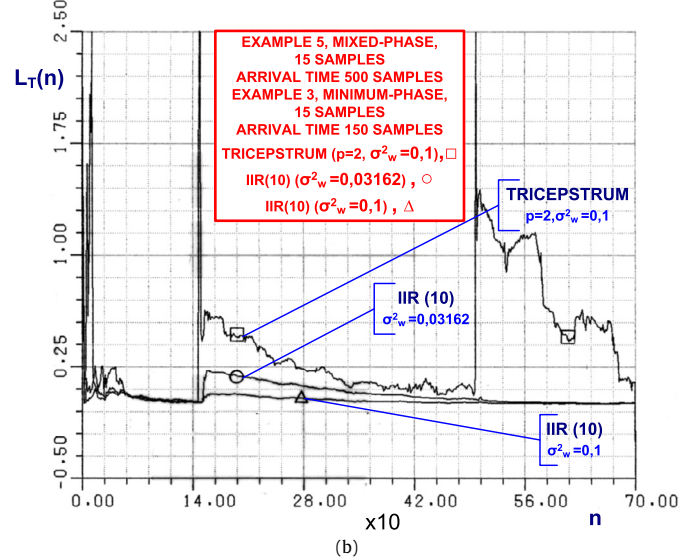
for the case of much higher SNR value ($\sigma_w^2 = 3.162 \times 10^{-2}$). In the second part of this experiment we insert the minimum-phase example 3, at 150 samples and the mixed-phase example 5, at 500 samples. The rest of the variables are the same as in the first part of this experiment, the order of the IIR is 10 and both signal lengths are now 15 samples. Since the 2nd signal is minimum phase when $\sigma_w^2 = 3.162 \times 10^{-2}$ the IIR method performs better than in the previous scenario (Fig. 8b).

Test Case 5 (Transients of unknown arrival time in AWGN).

Adaptive implementation: In this experiment we demonstrate the performance of the tricepstrum method in the presence of additive, non-Gaussian, i.i.d., zero mean noise. We use uniform distribution for the noise process and we test the case of one signal (example 4, 15 samples, arrival time 150 samples) and two signals (examples 4 and 3, 15 samples, arrival times 150, 350 samples). In Figs. 9a, 9b we show relative performance for $\sigma_w^2 = (0.7905) \times 10^{-1}, 0.025, \lambda = 0.99$ and orders 2 and 6 respectively for one signal. It is apparent that because the optimality of the IIR approach is based on the AWGN assumption its performance degrades, whereas the tricepstrum algorithm remains insensitive to the non-Gaussian noise and since in this case the fourth-order statistics become a much better SNR environment



(a)



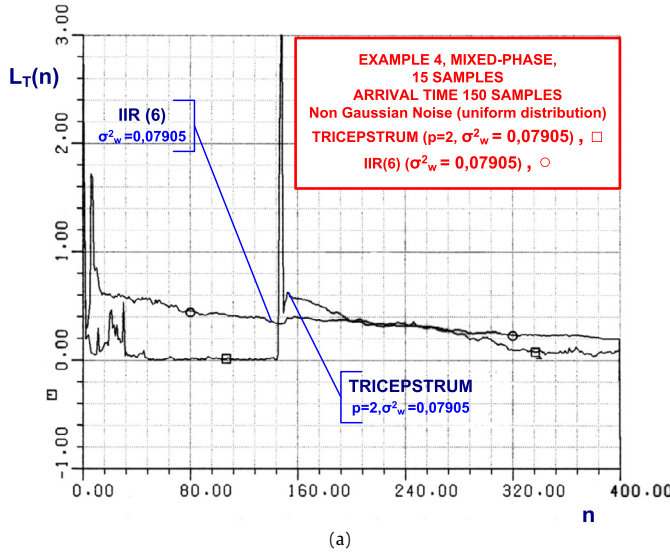
(b)

Fig. 8. Additive White Gaussian Noise, two signals: (a) mixed-phase, example 4, 15 samples, arrival time 150 samples and minimum-phase example 3, 25 samples, arrival time 350 samples, L_T versus time $\lambda = 0.99, \sigma_w^2 = 0.1, p = 2$ for Tricepstrum and $\sigma_w^2 = 0.1, 3.162 \times 10^{-2}$ for IIR(10), (b) minimum-phase, example 3, 15 samples, arrival time 150 samples and mixed-phase, example 5, 15 samples, arrival time 500 samples, L_T versus time, $\lambda = 0.99, \sigma_w^2 = 0.1, p = 2$ for Tricepstrum and $\sigma_w^2 = 0.1, \sigma_w^2 = 3.162 \times 10^{-2}$ for IIR(10).

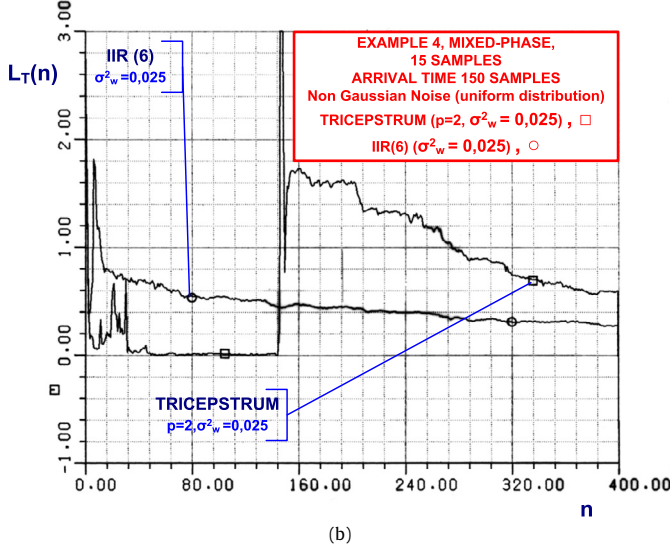
($\frac{E[X_G^4(n)]}{E[X_U^4(n)]} = \frac{240}{16a^2}$, where “G” stands for Gaussian and “U” for uniform $[-a/2, a/2]$) the tricepstrum method performs much better than in the AWGN case if we keep the noise variance constant. In the second part of this experiment we verify the same result using two signals in even lower SNR. In Figs. 10a, 10b the noise variance is $\sigma_w^2 = 1, 0.1, \lambda = 0.99$ and the orders of the models are 2 and 6 as before. Finally, in Fig. 11, we show R.O.C. curves for SNR = 15 dB, record length 150, arrival time 90, for white noise with exponential distribution of zero mean. The signal is example (5), 15 samples.

Test Case 6 (Unknown arrival time).

Adaptive Implementation: In this test we first demonstrate matching of the c.d.fs under H_1 for two examples when the arrival times of the transients are unknown. In Fig. 12a we show the case under H_0 , for 500 Monte-Carlo runs ($p = 2, l = 2$) and data record



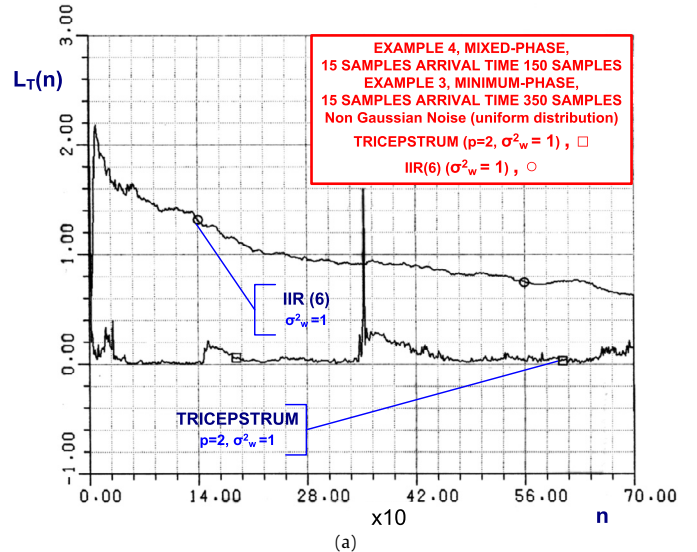
(a)



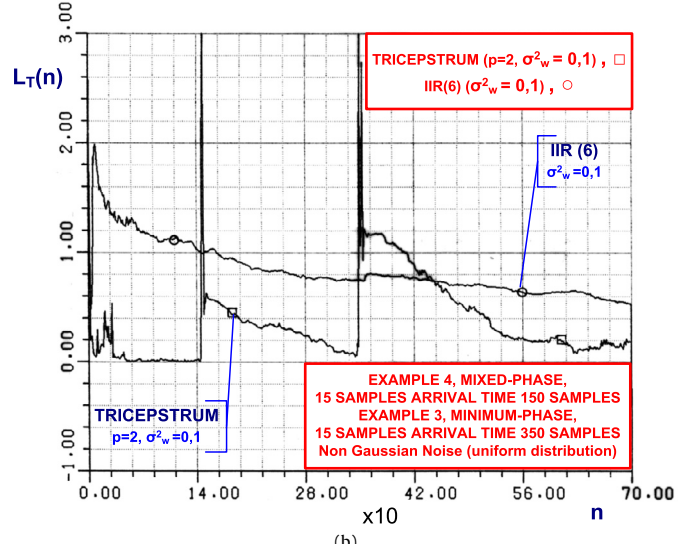
(b)

Fig. 9. Additive White non-Gaussian (uniform distribution) Noise, signal, mixed phase, example 4, 15 samples, arrival time 150 samples: (a) L_T versus time, $\lambda = 0.99$, Tricepstrum, $p = 2$ and IIR(6), $\sigma_w^2 = 0.7905 \times 10^{-1}$, (b) L_T versus time, $\lambda = 0.99$, $\sigma_w^2 = 0.025$.

length 150. We repeat the same comparison, Fig. 12b, 100 sample sequences under H_1 for example 1, SNR = 15 dB and arrival time at 90 samples. The record length is also 150 samples and the conditions for the tricepstrum detector are, $p = 2$, $l = 2$, $\lambda = 0.99$. Using a second signal, example 5, at SNR = 15 dB and for 100 sample sequences, in Fig. 12c we demonstrate the same matching of the c.d.fs. In this case the arrival time of the transient is at 150 samples and the record length is 250 samples. The specifications for the tricepstrum detector remain the same as in the previous test (example 1). The net conclusion from these figures is that there is a fairly close agreement. For both cases, signal length 15 samples. Next in this experiment we demonstrate insensitivity of the tricepstrum detection performance to the arrival time. In Fig. 12d we overlap R.O.C. curves for example (1) when the arrival time is known, at 0 samples and unknown at 90 samples. The record length is 150 samples and the SNR = 15 dB and for the same SNR for example (5), arrival time at 150 samples and record length 250 samples (for all cases $p = 2$, $l = 2$, $\lambda = 0.99$). Finally, in terms of R.O.C. curves we compare with the IIR based detector and we show in Fig. 12e performance for example (5) at



(a)



(b)

Fig. 10. Additive White non-Gaussian (uniform distribution) Noise, two signals, mixed-phase, example 4 and minimum-phase example 3, both 15 samples, arrival times, 150, 350, samples: (a) L_T versus time, $\lambda = 0.99$, Tricepstrum, $p = 2$ and IIR(6), $\sigma_w^2 = 1$, (b) L_T versus time, $\lambda = 0.99$, $\sigma_w^2 = 0.1$.

SNR = 15 dB, 20 dB and arrival time at 150 samples (record length 250), $\lambda = 0.99$. For the tricepstrum $p = 2$, $l = 2$ (Fig. 12).

Detection Performance in Additive White non-Gaussian Noise (AWNGN)

Higher order (3rd, 4th, etc.) cumulants are zero for Gaussian i.i.d. process [16]. This means that cumulants have the ability to suppress the noise. This fact is one of the reasons that we presented a detection statistic based on cepstrum coefficients and particularly the ones based on the tricepstrum sequence. However, the same detection statistic still works when noise is not Gaussian i.i.d. but non-skewed (e.g. symmetrically distributed).

This becomes apparent if we compare Fig. 8b, where the noise is Gaussian i.i.d. and Fig. 10b where the noise is non-Gaussian i.i.d. but of uniform distribution. Clearly the performance of the detection statistic is almost the same. The two experiments were conducted with the same SNR ($\sigma_w^2 = 0.1$ for both).

Now, if we try to compare the performance of the detection statistic when the noise is non-Gaussian with asymmetric distribution then, we have the result shown in Figs. 13a, 13b. In Fig. 13a we plot probability of detection versus probability of false alarm,

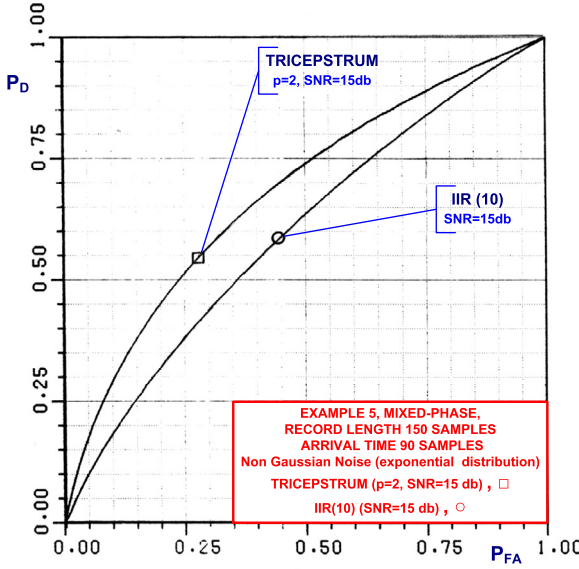


Fig. 11. Additive White non-Gaussian (exponential distribution) Noise, signal, mixed-phase, example 5, Probability of detection versus probability of false alarm, SNR = 15 dB, arrival time, 90 samples, record length 150 samples, Tricepstrum ($p = 2$), IIR(10), $\lambda = 0.99$.

for the signal of example 5 (mixed phase) with SNR 15 dB when the noise is non-Gaussian with exponential distribution and in Fig. 13b we plot the same probabilities, for the same signal with the same SNR but, the noise now is Gaussian. In the presence of non-Gaussian asymmetric noise the probability of detection is much less for the same probability of false alarm, than the corresponding number in the Gaussian case.

Next we study the behavior of the tricepstrum detector when the noise is non-Gaussian i.i.d. with the following p.d.fs.

$$1) f(x) = (1 - \varepsilon) \frac{e^{-x^2}}{(2\pi\sigma_0^2)^{\frac{1}{2}}} + (\varepsilon) \frac{e^{-x^2}}{(2\pi\sigma_1^2)^{\frac{1}{2}}}, \text{ contaminated Gaussian}$$

where, $\varepsilon = 0, 2$, $\sigma_0^2 = 0, 25$ is the nominal variance, $\sigma_1^2 = 4$ is the contaminated noise variance ($\sigma_1^2 > \sigma_0^2$), $0 \leq \varepsilon \leq 1$ is the degree of contamination.

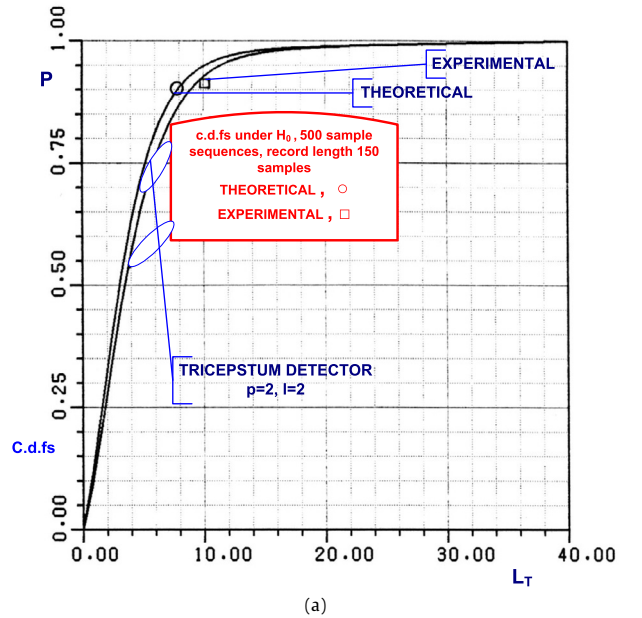
$$2) f(x) = \frac{\sigma}{\pi(\sigma^2 + x^2)}, \text{ Cauchy, signal energy equals 250 and } \sigma = 1.$$

Those non-Gaussian p.d.fs. are commonly used to model impulsive noises. In radar, sonar and communication applications, ideal signals are usually contaminated with impulsive noises. For example lighting impulsive noise significantly reduces the signal detector performance by 25%.

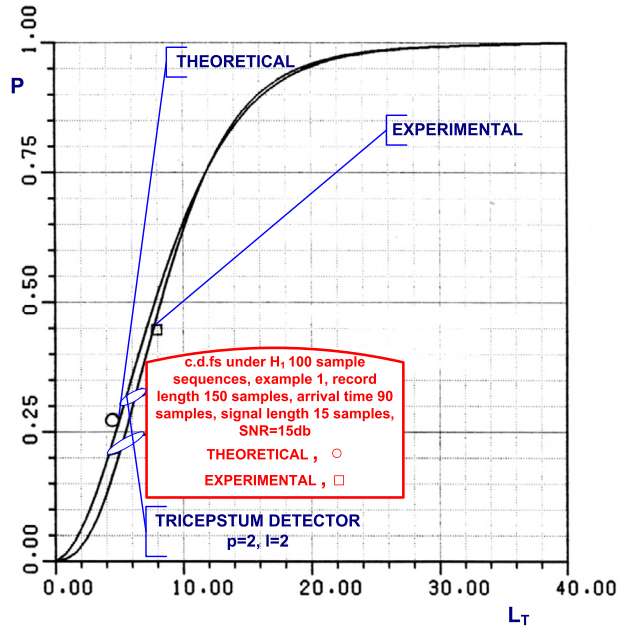
In Figs. 14a and 14b we demonstrate the matching of the c.d.fs when the noise is non-Gaussian of either type of the two above, under H_1 for example 3. Similarly we compare the behavior of the tricepstrum detector in terms of R.O.C. curves in Figs. 14c and 14d when, the noise is Gaussian and when the noise follows the above two aforementioned non-Gaussian models.

Test Case 7 (Real Data).

Adaptive Implementation: In this example real data of length 512 samples per record were used ($p = q = 4$). Fig. 15 shows the evolution of the decision statistic L_T with time for the adaptive implementation under both hypothesis H_0 and H_1 . We observe that the separation of the two learning curves is clear even though the SNR is close to 0 dB.



(a)

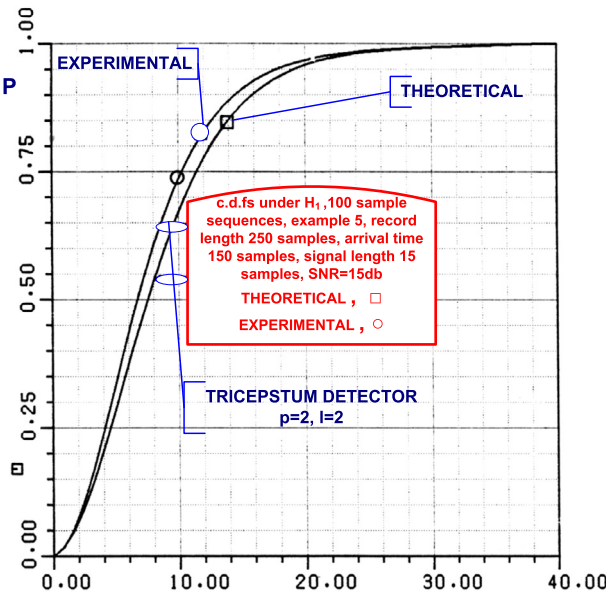


(b)

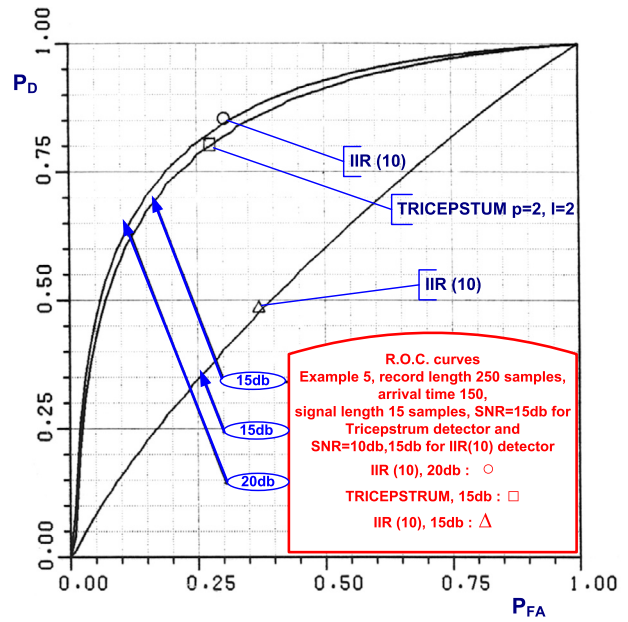
Fig. 12. Additive White Gaussian Noise: c.d.fs. under H_0 , 500, sample sequences, record length 150 samples, theoretical and experimental distribution functions, (b) example 1, under H_1 , SNR = 15 dB, arrival time at 90 samples, record length 150 samples, (c) example 5, under H_1 , SNR = 15 dB, arrival time at 150 samples, record length 250 samples, $p = 2$, $l = 2$, $\lambda = 0.99$ for both (b) and (c), (d) R.O.C curves for examples 1, 5. The same conditions as in (b) and (c) are used, (e) R.O.C curves for example 5, Tricepstrum $p = 2$, $l = 2$, and SNR = 15dB, IIR(10), SNR = 15 dB, 20 dB. The rest of the conditions as in (c).

4. Conclusion

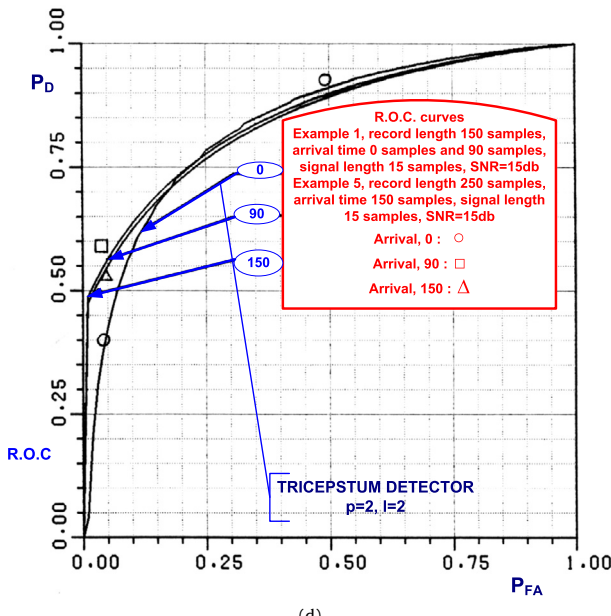
Using a suitable partition of the fourth order statistics involved in (2), a recursive solution for the cepstral equation was formulated. Because of the high variance in the estimation of the fourth order statistics the recursive approach was based on orthogonal Q-R decompositions of the partitioned data matrices which consist the cepstral equation. By means of simulation examples it was demonstrated that the proposed algorithm is capable to detect transients of unknown arrival times. Comparing this technique with a fast adaptive algorithm based on an IIR model for the signal,



(c)



(e)



(d)

Fig. 12. (continued)

significant improvement in terms of signal detection capability was demonstrated. When the theoretical cumulative distributions under H_1 were compared to the experimental ones they were found to be in close agreement. This was the case for both, AWGN and AVNGN. The detection statistic is insensitive to non-Gaussian i.i.d. noise, if it is non-skewed (e.g., symmetrically distributed). On the contrary, when the noise is non-Gaussian i.i.d. but, with asymmetrical distribution we experienced deterioration in its performance. The property of the tricepstrum detector to be sensitive to non-minimum phase signals was also shown. The proposed method is essentially designed for unknown arrival times, which includes the case of known arrival of the transients, it is a constant false alarm (CFAR) detector and there is no need for any a-priori information of the signal. Finally, it was shown that the tricepstrum based detector is insensitive to the arrival time of the transients, as long as the adaptive algorithm under H_0 has adjusted itself to the noise level.

Appendix A

A.1. Comment on the convergence of the recursive approach

If we assume stationary input statistics with zero mean and using the same steps as in [25,32] convergence of the cepstrum coefficient vector in the mean and mean square can be shown.

A.2. Exponential initial convergence

From (6) substituting (14) we have,

$$\mathbf{F}(p, n)\mathbf{T}(p, n) = \mathbf{F}(p, n)\mathbf{T}(p, n - 1) + \mathbf{F}(p, n)\mathbf{F}^{-1}(p, n)(\mathbf{a}^T(n) - \mathbf{A}(p, n)\mathbf{T}(p, n - 1)) \quad (\text{A.1})$$

since,

$$\mathbf{F}(p, n) = \lambda \cdot \mathbf{F}(p, n - 1) + \mathbf{A}(p, n) \quad (\text{A.2})$$

we obtain,

$$\mathbf{F}(p, n)\mathbf{T}(p, n) = \lambda \cdot \mathbf{F}(p, n - 1)\mathbf{T}(p, n - 1) + \mathbf{a}^T(n), \quad (\text{A.3})$$

and subtracting from both sides of (A.3) the product, $\mathbf{F}(p, n)\bar{\mathbf{T}}(p, n)$,

$$\mathbf{F}(p, n) \cdot \Delta\mathbf{T}(p, n) = \lambda \cdot \mathbf{F}(p, n - 1) \cdot \Delta\mathbf{T}(p, n - 1) + \mathbf{a}^T(n) - \mathbf{A}(p, n)\bar{\mathbf{T}}(p, n), \quad (\text{A.4})$$

where, $\Delta\mathbf{T}(p, n) = \mathbf{T}(p, n) - \bar{\mathbf{T}}(p, n)$ and we made use of (A.2). Rewriting (A.4) in terms of the initial time n_0 we have,

$$\mathbf{F}(p, n) \cdot \Delta\mathbf{T}(p, n) = \lambda^{n-n_0} \cdot \mathbf{F}(p, n_0) \cdot \Delta\mathbf{T}(p, n_0) - (\mathbf{F}(p, n)\bar{\mathbf{T}}(p, n) - \mathbf{C}(p, n)), \quad (\text{A.5})$$

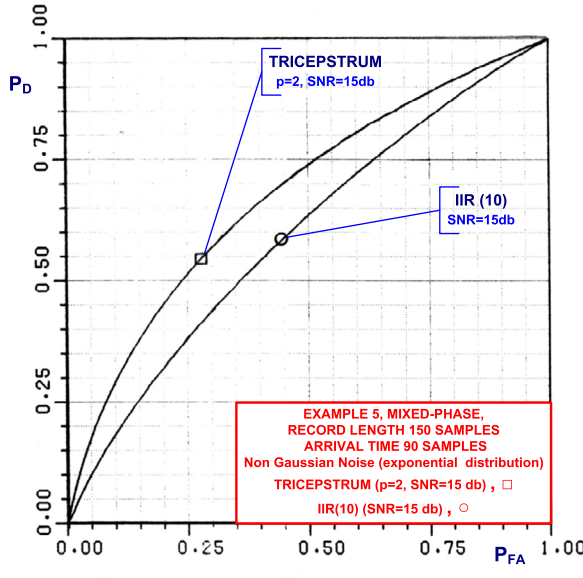
and taking expectations,

$$E\{\Delta\mathbf{T}(p, n)\} = \lambda^{n-n_0} E\{\mathbf{F}^{-1}(p, n)\mathbf{F}(p, n_0)\} \Delta\mathbf{T}(p, n_0) - (\bar{\mathbf{T}}(p, n) - E\{\mathbf{F}^{-1}(p, n)\mathbf{C}(p, n)\}) \quad (\text{A.6})$$

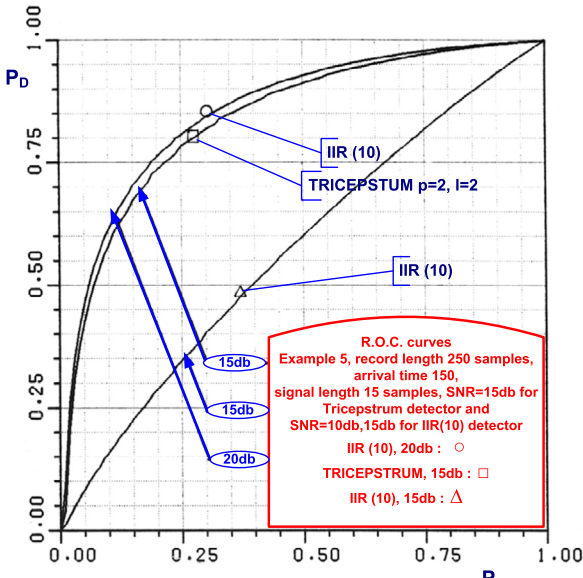
Substituting $\bar{\mathbf{T}}(p, n) \simeq \bar{\mathbf{F}}^{-1}(p, n)\bar{\mathbf{C}}(p, n)$, we obtain,

$$E\{\Delta\mathbf{T}(p, n)\} = \lambda^{n-n_0} \cdot E\{\mathbf{F}^{-1}(p, n)\mathbf{F}(p, n_0)\} \cdot \Delta\mathbf{T}(p, n_0). \quad (\text{A.7})$$

This shows the exponential nature of the initial convergence [33].



(a)



(b)

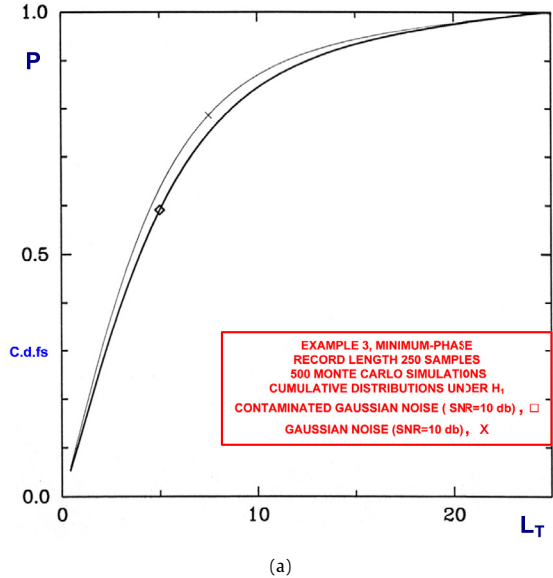
Fig. 13. R.O.C curves for non-Gaussian (exponential distribution) and Gaussian distribution of noise: (a) probability of detection versus probability of false alarm, for the signal of example 5 (mixed phase) with SNR 15 dB when the noise is non-Gaussian with exponential distribution, (b) same conditions as in (a) but the noise is Gaussian.

Appendix B

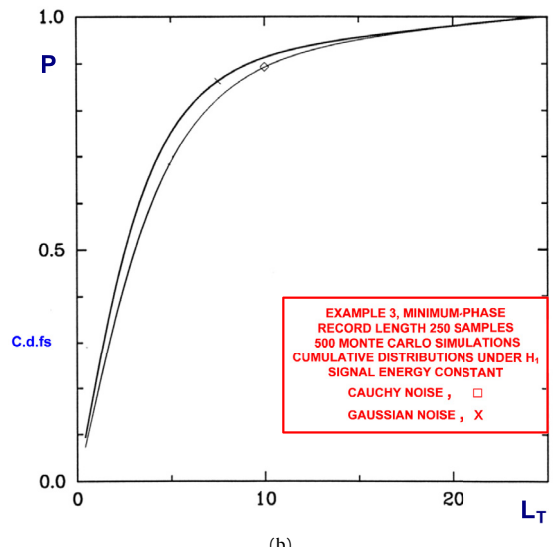
From (2) and if there is no noise present, we have for $0 \leq m \leq 2p$, $m \neq p$,

$$f_m(m, k) = \sum_{q,j,v=1}^M B(q, j, v) e^{(b_q + b_j + b_v)(m-k)} e^{-(b_q + b_j + b_v)p} \cdot [e^{(b_j + b_v)k} - 1] e^{2(b_q + (b_j + b_v))p}, \quad 1 \leq k \leq p, \quad (\text{B.1})$$

$$f'_m(m, k) = \sum_{q,j,v=1}^M B(q, j, v) e^{(b_q + b_j + b_v)(m-k)} e^{-(b_q + b_j + b_v)p} \cdot [e^{(b_j + b_v)p} - e^{(b_j + b_v)k}] e^{b_q p}, \quad p+1 \leq k \leq 2p, \quad (\text{B.2})$$



(a)



(b)

Fig. 14. Matching of the c.d.fs and R.O.C curves for non-Gaussian (Contaminated Gaussian and Cauchy) and Gaussian distribution of noise: (a) matching of c.d.fs for example 3 (minimum phase) when the noise is Contaminated Gaussian and Gaussian, (b) matching of c.d.fs for example 3 (minimum phase) when the noise is Cauchy and Gaussian, (c) matching of R.O.C curves for example 3 (minimum phase) when the noise is Contaminated Gaussian and Gaussian, (d) matching of R.O.C curves for example 3 (minimum phase) when the noise is Cauchy and Gaussian.

where

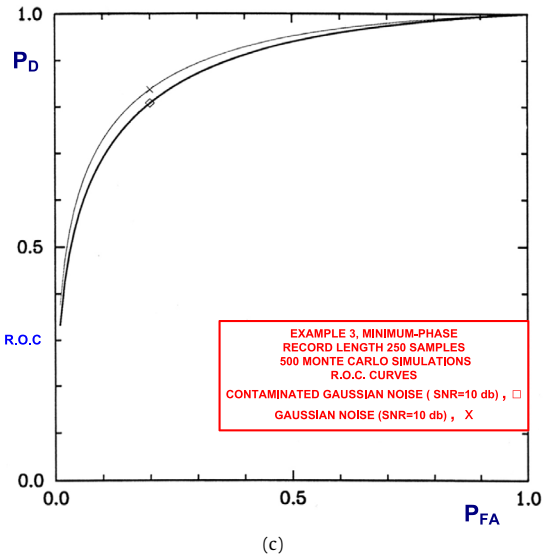
$$B(q, j, v) = \sum_{q,j,v=1}^M h_i h_q h_j b_v [1/(1 - e^{b_i + b_q + b_j b_v})]. \quad (\text{B.3})$$

Then the matrix $\mathbf{F}(p, n)$ can be decomposed as,

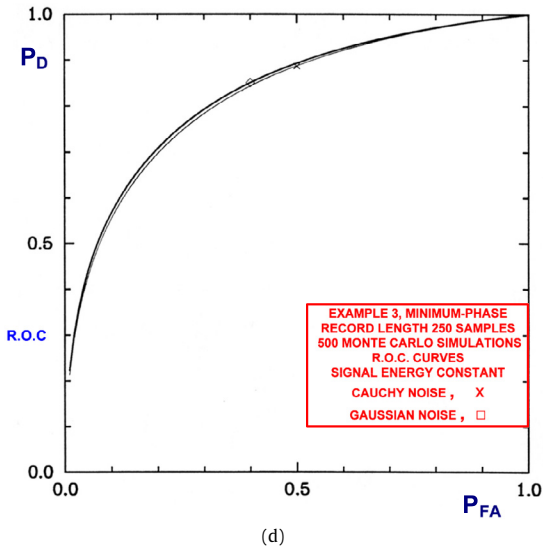
$$\mathbf{F}(p, n) = \mathbf{W}_{2px\hat{M}} \cdot \mathbf{B}_{\hat{M}x\hat{M}} \cdot \mathbf{R}_{\hat{M}x\hat{M}} \cdot \mathbf{T}\mathbf{X}_{\hat{M}x2p}, \quad n \rightarrow \infty \quad (\text{B.4})$$

where,

$$\mathbf{W} = \begin{pmatrix} 1 & 1 & \dots & 1 \\ t_1 & t_2 & \dots & t_{\hat{M}} \\ \vdots & \vdots & \ddots & \vdots \\ t_1^{2p} & t_2^{2p} & \dots & t_{\hat{M}}^{2p} \end{pmatrix}, \quad (\text{B.4.1})$$

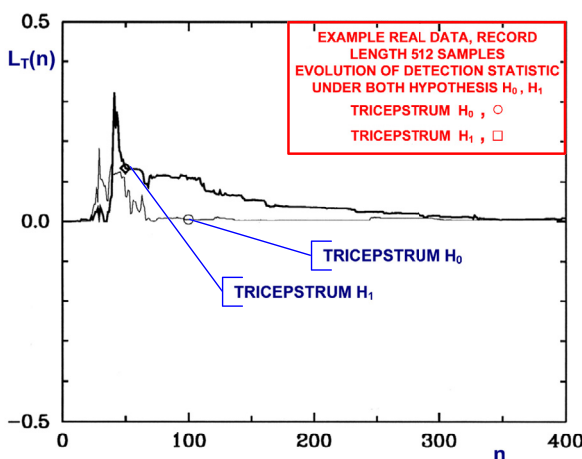


(c)



(d)

Fig. 14. (continued)

Fig. 15. Real data record, length 512 samples, evolution of detection statistic L_T under both hypothesis H_0 and H_1 .

$$\mathbf{B} = \text{diag}[B(q, j, v)], \quad (B.4.2)$$

$$\mathbf{R} = \text{diag}[t_1^{-p}, t_2^{-p}, \dots, t_{\hat{M}}^{-p}], \quad (B.4.3)$$

$$\mathbf{TX} = \begin{pmatrix} t_1^{-1}x_1 & \dots & t_1^{-p}x_1 & t_1^{-(p+1)}y_1 & \dots & t_1^{-2p}y_1 \\ t_2^{-1}x_2 & \dots & t_2^{-p}x_2 & t_2^{-(p+1)}y_2 & \dots & t_2^{-2p}y_2 \\ \vdots & \ddots & \vdots & \vdots & \ddots & \vdots \\ t_{\hat{M}}^{-1}x_{\hat{M}} & \dots & t_{\hat{M}}^{-p}x_{\hat{M}} & t_{\hat{M}}^{-(p+1)}y_{\hat{M}} & \dots & t_{\hat{M}}^{-2p}y_{\hat{M}} \end{pmatrix}, \quad (B.4.4)$$

$$t_{q,j,v} = e^{(b_q + b_j + b_v)}, \quad \hat{M} = M^2$$

$$q = 1, 2, \dots, \hat{M}; \quad j = q, \dots, \hat{M}; \quad v = j, \dots, \hat{M},$$

and $x_i y_i$ are inner products of vectors of the form,

$$(a_k e^{A_k b_k} \beta_k e^{B_k b_k} \gamma_k e^{F_k b_k}), \quad k = 1, 2, \dots, M, \quad (B.5)$$

which are all linearly independent and therefore \mathbf{TX} has rank $2p$ if $2p \leq M$. The above decomposition was drawn from [34,35].

References

- [1] B. Porat, B. Friedlander, Adaptive detection of transient signals, *IEEE Trans. Acoust. Speech Signal Process.* 34 (December 1986) 1410–1418.
- [2] B. Friedlander, B. Porat, Detection of transient signals by the Gabor representation, *IEEE Trans. Acoust. Speech Signal Process.* 37 (February 1989) 169–179.
- [3] A. Polydoros, C.L. Nikias, Detection of unknown frequency sinusoids in noise, *IEEE Trans. Acoust. Speech Signal Process.* 35 (June 1987) 897–900.
- [4] J.W. Ketchum, D. Herrick, Signal detection using autoregressive parameters, in: *ICASSP'85*, Tampa, Florida, April 1985, pp. 9.8.1–9.8.4.
- [5] E.K.L. Hung, R.W. Herring, Simulation experiments to compare the signal detection properties of DFT and MEM spectra, *IEEE Trans. Acoust. Speech Signal Process.* 29 (October 1981) 1084–1089.
- [6] W.S. Burdic, Detection of narrowband signals using time domain adaptive filters, *IEEE Trans. Aerosp. Electron. Syst.* 14 (July 1978) 578–591.
- [7] M. Sanaullah, A review of higher order statistics and spectra in communication systems, *Glob. J. Sci. Front. Res., Phys. Space Sci.* 13 (4) (2013), version 1.0 year.
- [8] Jean-Marc Le Caillec, Rene Garello, Asymptotic bias and variance of conventional bispectrum estimates for 2-D signals, *Multidimens. Syst. Signal Process.* 16 (2005) 49–84.
- [9] B. Liang, S.D. Iwnicki, Y. Zhao, Application of power spectrum, cepstrum, higher order spectrum and neural network analyses for induction motor fault diagnosis, *Mech. Syst. Signal Process.* 39 (2013) 342–360.
- [10] F. Gu, et al., Electrical motor current signal analysis using modified bispectrum for fault diagnosis of downstream mechanical equipment, *Mech. Syst. Signal Process.* 25 (2011) 360–372.
- [11] Mohammed A. Hassan, David Coats, Kareem Gouda, Yong-June Shin, Abdel Bayoumi, Analysis of nonlinear vibration-interaction using higher order spectra to diagnose aerospace system faults, in: *IEEE Aerospace Conference*, March 2012, Paper #1345, version 4.
- [12] Bo Liang, The higher order spectrum analysis for fault pattern extraction of induction motors, in: *9th International Conference on Power Electronics and ECCE Asia, ICPE-ECCE Asia*, June 2015.
- [13] Anjan Gudigara, Shreesha Chakkadai, U. Raghavendra, U. Rajendra Acharyab, Local texture patterns for traffic sign recognition using higher order spectra, *Pattern Recognit. Lett.* 94 (July 2017) 202–210.
- [14] U. Rajendra Acharya, Vidya K. Sudarshana, Joel E.W. Koha, Roshan Joy Martisd, Jen Hong Tana, Shu Lih Oha, Adam Muhammada, Yuki Hagiwarraa, Muthu Rama, Krishanan Mookiah, Application of higher-order spectra for the characterization of coronary artery disease using electrocardiogram signals, *Biomed. Signal Process. Control* 31 (January 2017) 31–43.
- [15] R. Pan, C.L. Nikias, The complex cepstrum of higher-order cumulants and non-minimum phase system identification, *IEEE Trans. Acoust. Speech Signal Process.* 36 (February 1988) 186–205.
- [16] C.L. Nikias, M.R. Raghuveer, Bispectrum estimation: a digital signal processing framework, *Proc. IEEE* 75 (July 1987) 869–891.
- [17] C.L. Nikias, ARMA bispectrum approach to nonminimum phase system identification, *IEEE Trans. Acoust. Speech Signal Process.* 36 (April 1988) 513–524.
- [18] T. Matsuoka, T.J. Ulrych, Phase estimation using the bispectrum, *Proc. IEEE* 72 (1984) 1403–1411.
- [19] K.S. Lii, M. Rosenblatt, Deconvolution and estimation of transfer function phase and coefficients for non-Gaussian linear processes, *Ann. Stat.* 10 (1982) 1195–1208.

- [20] D. Kletter, M. Messer, Detection of non-Gaussian signal in Gaussian noise using higher-order spectral analysis, in: Proc. Workshop on Higher-Order Spectral Analysis, Vail, CO, June 1989, pp. 95–99.
- [21] M.J. Hinich, C. Wilson, Detection of non-Gaussian signals in non-Gaussian noise using bispectrum, *IEEE Trans. Acoust. Speech Signal Process.* 38 (7) (July 1990) 1126–1131.
- [22] P. Nicolas, D. Kraus, Detection and estimation of transient signals in colored Gaussian noise, in: ICASSP'88, New York, April 1988, pp. 2821–2824.
- [23] M.J. Hinich, Detecting a transient signal by bispectral analysis, *IEEE Trans. Acoust. Speech Signal Process.* 38 (July 1990) 1277–1283.
- [24] M.J. Hinich, M.A. Wolinski, A test for aliasing using bispectral analysis, *J. Am. Stat. Assoc.* 83 (June 1988) 499–502.
- [25] S. Haykin, *Adaptive Filter Theory*, Prentice-Hall, Englewood Cliffs, NJ, 1986.
- [26] A.P. Petropulu, C.L. Nikias, The complex cepstrum and bispectrum: analytic performance evaluation in the presence of Gaussian noise, *IEEE Trans. Acoust. Speech Signal Process.* 38 (July 1990) 1246–1256.
- [27] J. Makhoul, Linear prediction: a tutorial review, *Proc. IEEE* 63 (April 1975) 561–580.
- [28] J.J. Dongarra, C.B. Moler, J.R. Bunch, G.W. Stewart, *LINPACK User's Guide*, SIAM, Philadelphia, 1979.
- [29] B. Porat, B. Friedlander, On the accuracy of the kumaresan tufts method for estimating complex damped exponentials, *IEEE Trans. Acoust. Speech Signal Process.* 35 (February 1987) 231–235.
- [30] S.M. Kay, Robust detection by autoregressive spectrum analysis, *IEEE Trans. Acoust. Speech Signal Process.* 30 (April 1982) 256–269.
- [31] C. Carayannis, D.G. Manolakis, N. Kalouptsidis, A fast sequential algorithm for least-squares filtering and prediction, *IEEE Trans. Acoust. Speech Signal Process.* 31 (December 1983) 1394–1402.
- [32] F. Ling, J.G. Proakis, Non stationary learning characteristics of least squares adaptive estimation algorithms, in: Proc. ICASSP'84, San Diego, March 1984, pp. 7.3.1–7.3.4.
- [33] E. Eleftheriou, D.D. Falconer, Tracking properties and steady-state performance of the RLS adaptive algorithms, *IEEE Trans. Acoust. Speech Signal Process.* 34 (October 1986) 1097–1109.
- [34] D. Tufts, R. Kumaresan, Estimation of frequencies of multiple sinusoids: making linear prediction perform like maximum likelihood, *Proc. IEEE* 70 (1982) 975–989.
- [35] C. Papadopoulos, C.L. Nikias, Parameter estimation of exponentially damped sinusoids using higher order-statistics, *IEEE Trans. Acoust. Speech Signal Process.* 38 (August 1990) 1424–1436.

Christos K. Papadopoulos, was born in Athens, Greece. He received the Diploma degree in electrical and computer engineer from the department of electrical and computer engineering of the polytechnic school of Aristotelian University of Thessaloniki, Greece in 1984 and the M.S. and Ph.D. degrees in Communication and Digital Signal Processing from the Dept. of electrical and computer engineering of Northeastern University, U.S.A, Boston, M.A. in 1987 and 1991 respectively. 1985 to 1990 was a Teaching and Research Assistant at Northeastern University. 1990 to 1991 with Digital Measurement Systems Corp. Burlington, Boston, M.A. 1993 to 1997 with SIEMENS S.A. Athens, Greece. 1997 to 2009 with ANCO S.A. Athens, Greece. 2009–till today Lecturer in Piraeus University of Applied Sciences, Electrical Engineering Department. His research interests are in digital signal processing and adaptive algorithms.

George Ioannidis was born in Athens, Greece, in 1970. He received the Diploma and the Ph.D. degree in electrical engineering both from National Technical University of Athens in 1993 and 1998 respectively. He is currently a Professor in the Department of Electrical Engineering of the Piraeus University of Applied Sciences. His main research interests concern dc–dc and dc–ac converters (power topology and control), dc and ac drives, energy saving applications and signal processing.

Dr. Constantinos Psomopoulos, graduated as an Electrical and Computers Engineer at the School of Electrical and Computers Engineering, National Technical University of Athens Greece in 1997 and received his Ph.D. from the same School in 2002. Since 2007 he is member of Academic Staff in Piraeus University of Applied Sciences, Electrical Engineering Department where now he is Vice President. He has worked for several years in different industrial sectors and he is now an independent consultant and inspector in these infrastructures regarding operation, risks assessment, damage evaluation and recovery after faults. He is member of the research team of EEC Columbia University NY. He is a certified expert in Critical Energy Infrastructures Protection according to 2008/114/ EC Directive.